UNIVERSITY OF PISA

Engineering Ph.D. School "Leonardo da Vinci"

Ph.D. course in Chemical and Material Engineering

XXIV cycle

Realization and characterization of bioactive composite materials for locomotor tissue regeneration

ING-IND34

Tutor

Eng. Giovanni Vozzi

Prof. Giuliano Cerulli

PhD student

Francesca Montemurro

2011/2012

Abstract

Tissue Enginnering emerges as a potential and alternative therapeutic process to treat severely injured patients with minimally invasive techniques. Cartilage and bone injuries occur due to several reasons and they compromise quality of life. This thesis was focused on development of biomaterials that could mimic cartilage and bone tissue, using only natural substances, gelatin and/or collagen, crosslinked with genipin (GP) and hydroxyapatite (HA) . These materials are cheap and easy to handle, and in particular collagen, represents a chemoattractor factor, that may help cellular colonization. First of all genipin reaction was studied to establish reaction rate constant and crosslinking degree as function of genipin concetrations. The optimal genipin concentration was decided primarly assuring that it was not cytotoxic, meseauring its release in acqueous enviroment. Then elastic moduli of scaffolds prepared with different GP concentrations, different protocols and different HA concentrations were measured taking into account that scaffolds had to present mechanical properties suited to the implant site. Roughness surface of scaffolds, was also investigated with SEM, to ensure an optimal integration with implant site and to verify the presence of a right porosity to allow its cell colonisation. Bone scaffolds were arranged to reproduce a HA gradient, an important bone feature, and their anisotropy was valueted. Biocompatibility tests, *in vitro* tests, for cartilage and bone biomateri-

als were performed using primary and immortalised cells. Finally preliminary *in vivo* tests using small animal models, rats with a femur lesion, were performed for cartilage and bone substitute, selected on the basis of their mechanical properties. The aim was to follow bone and cartilage regeneration, after injection of biomaterials, and to compare it with the physiological regeneration.

Acknowledgements

Ed ora la parte più difficile per me....Siccome ormai inizio ad avere una “certa età”, e le persone da ringraziare sono tante, mi scuso da subito se dimentico qualcuno. Inizio ringraziando i tutor: Giovanni Vozzi per aver creduto in me sin dall'inizio e per avermi voluto nel “regno” del Centro Piaggio, e soprattutto per avermi introdotto e svelato il mondo della Bioingegneria; il Professor Cerulli per avere sostenuto e reso possibile tutto questo lavoro di ricerca attraverso la Nicola's Foundation e la Let People Move; il co-tutor Dott. Claudio Domenici, che mi ha ospitato nel fondamentale laboratorio della Fisiologia Clinica del CNR e che ha diviso con me i suoi buoni pasto della mensa (anche se il risotto con gli spinaci e un pò di sugo sopra è la negazione della cucina mediterranea!!!). Ringrazio la Prof. Arti Ahluwalia per i suoi continui stimoli e preziosi consigli, poi tutto l'MCB group (Ma Che Bel gruppo!!!): naturalmente inizio con Tita (per gli amici Annalisa) spalla lavorativa ed extra-lavorativa, che mi ha supportato e sopportato, poi il compagno di avventura di PhD Carmelo (l'altra metà del neurone...), il Vozzino (Federico) amico di lunga data, che mi ha svelato tutti i segreti del mondo cellulare, Serena che riesce sempre a risollevare le giornate degli altri (non volendo) con i suoi piccoli inghippi....Continuo con l'Elbano (Daniele) e le sue perle di saggezza, Tommy “il diplomatico”, Giorgi(o) ed i suoi fegatelli, Gianni e il silicone, Nadia e il suo tentativo di ordinare il lab, l'italiano Yudano, la

dott.ssa Vinci la donna più impegnata del mondo. Ringrazio la Dott.ssa Monica Mattioli Belmonte e Concetta per l'ospitalità riservatami in quel di Ancona e per il fondamentale apporto nella parte biologica di questo lavoro. Ugualmente importanti sono stati gli amici (Dina in primis) e la valvola di sfogo extralavorativa, il calcetto con tutte le ragazze ed i mister che si sono succeduti nel tempo. Infine, naturalmente ringrazio tutta la mia famiglia per avermi sostenuto in tutto e per tutto. Grazie a tutti.

Francesca

Contents

List of Abbreviations

A Agar

ACC Agar and crosslinked collagen

AHA agar hydroxyapatite

ANCC Agar and not crosslinked collagen

ANCCHA agar+not crosslinked collagen+HA

BSA Bovine serum albumin

Ca-P calcium phosphate

CC Collagen Constructs

CPD critical point drying

DAPI 4',6-diamino-2-phenyldione

DMEM Dulbecco's Modified Eagle's Medium

DMSO Dimethyl sulfoxide

ECM extra-cellular matrix

EDC 1-ethyl-3-(3-dimethyl aminopropyl)-carbo-diimide

G gelatin and genipin

GAG glycosaminoglyan

GHA gelatin+HA crosslinked with genipin

GNCC gelatin and genipin with not crosslinked collagen

GNCCHA gelatin+not crosslinked collagen+HA

GPCC gelatin and genipin with pre crosslinked collagen

HA hydroxyapatite

NHS N-hydroxysuccinimide

PBS phosphate buffered saline

PEG poly(ethylene glycol)

PEO polyethylenoxide

PGA poly(glycolic acid)

PLA poly(D,L-lactic acid)

PLGA poly(lactic-co-glycolic acid)

PO propylene oxide

SEM Scanning electron microscopy

SEM-EDX Scanning electron microscopy-energy dispersive xray micro-analysis

TCP tricalcium phosphate

TE Tissue Engineering

List of Figures

List of Tables

1

Bone and cartilage

Introduction

Cartilage and bone injuries occur due to several reasons including degenerative, surgical, and traumatic processes, which significantly compromise quality of life and for this reason, they have long presented a challenge to physicians. Currently, millions of patients are suffering from bone and cartilage defects. Attention is focused especially on cartilage that has a reduced capacity to repair, due to the low mitotic activity of chondrocytes. On the contrary, bone has a high self repair capacity but for a large bone defect a surgical intervention is often required. In this chapter some traditional clinic techniques with their advantages and disadvantages, and the promising development of Tissue Engineering (TE) for bone and cartilage will be described. TE represents as a potential alternative therapeutic process to treat severely injured patients with minimally invasive techniques. Many and different are the materials used to obtain a suited biomaterial for bone and cartilage, this work is focused only on the use of natural components gelatin, collagen, hydroxyapatite (HA) and genipin. These materials are easy to obtain, to process, to sterilize and to handle in the surgical room (without preparation procedures, thus avoiding risks of infection).

1.1 Cartilage

1.1.1 Cartilage defects

In 1743, the famous English anatomist William Hunter wrote *'an ulcerated cartilage is a trouble-some problem... that, once destroyed, it is not recovered'* [1]. Why so many problems derives from a cartilage damage? This is a tissue that has a low self-repair capacity due to its particular and unique features: it is predominantly composed of a unique extra-cellular matrix (ECM), made of proteoglycans, negatively charged glycosaminoglyan (GAG) chains that swell and hydrate cartilage, and collagen type II, a fibrillar collagen that traps the proteoglycans and provides tensile strength. The biomecanical properties derive from ECM, and to regain a functional joint, cartilage defects would ideally be replaced by tissue of this precise composition. After a damage, which does not penetrate to the subchondral bone, intrinsic cartilage repair has different barriers: it is avascular, meaning that the nutrients required for energetic repair processes and the removal of metabolic waste products are limited by diffusion to / from surrounding tissues. It is relatively acellular; therefore few cells are available to affect repair [2]. These obstacles conspire to limit repair of defects to a fibrocartilaginous substitute tissue with different molecular composition (more type I collagen, less proteoglycan) and biomechanical behaviour (less proteoglycan and collagen type II, more collagen type I), compared with the original hyaline tissue [3]. On the contrary, a full-thickness (osteochondral) defect goes through the subchondral bone, accessing the bone marrow cells, including mesenchymal stem cells and also growth factors and cytokines [4]. The repair consists in the formation of a fibrocartilaginous tissue in the defect void. The events leading up to the formation of the repair tissue in a rabbit model have been characterised, indicating an immediate response to penetration of the subchondral bone in a full thickness defect with, in some cases, formation of hyaline-like articular cartilage[5]. This repair tissue is a poor substitute for articular cartilage, and a degeneration of both repaired and adjacent native tissues will be often observed after long-term follow-up (figure 1.1.1) [6].

Today, cartilage damage is still an issue for physicians and patients, and there is still no universally accepted and successful treatment approach for damaged

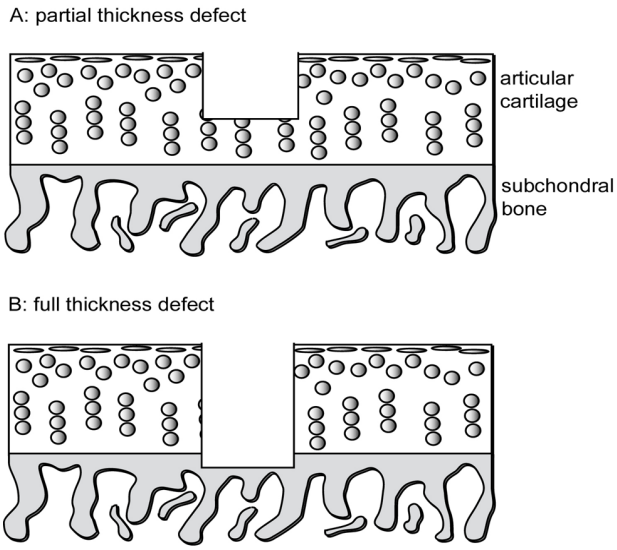

Figure 1.1.1: *A partial thickness focal defect in articular cartilage (A) and a full thickness defect involving the subchondral bone (B).*

cartilage. The common treatmentes for cartilage includes [7]:

- arthroscopic debridement, in which loose cartilage is trimmed;
- microfracture, in which bone marrow based repair is stimulated;
- autologous osteochondral grafting, in which bone-cartilage plugs are harvested from non-weight bearing joint sites and implanted directly into the defect;
- autologous chondrocyte implantation , a two-stage procedure involving harvest of chondrocytes, growth in vitro, then reimplantation.

These therapies were unsuccessful for a long term repair, they showed many side effects and they were limited to small lesions.

1.1.2 Tissue engineering

Tissue engineering has emerged as a new multidisciplinary field, that joins the latest developments in cell/molecular biology, materials science and engineering, chemistry and medical sciences towards the development of hybrid substitutes. These are obtained combining biodegradable supports (scaffolds), cells and signalling molecules, such as growth factors, aimed at restoring tissue or organs functions, using the natural signalling pathways and components of the organism [8]. Tissue engineering strategies have potential to be used in the regeneration of a series of tissues and organs and are especially adequate for the regeneration of articular cartilage, due to its own limited repair capacity. A critical requirement is the correct choice of the materials and the design of the scaffold structure. Even for a single tissue, the 'ideal scaffold' does not yet exist, and much more investigative work is needed on different materials combinations, the effect of porosity (porosity content, pore size distribution and interconnectivity), adequate cell sources and the best delivery strategies for growth factors [9]. Scaffolds will provide a shape, drive tissue development and permit the convenient delivery of cells into patients, it should be biodegradable and the degradation rate should match the extracellular matrix produced. Generically, three-dimensional (3D) porous scaffolds or hydrogels are the most widespread solutions for constructs, due to the high standard of cellular attachment and mechanical stability that is attained. The macrostructure of the scaffolds plays an important role also on the proliferation and migration of seeded cells into the matrix. Many types of materials have been proposed for both cartilage tissue engineering, most of them biocompatible and biodegradable polymers. Here they are grouped on the the basis of their different origin. Natural polymers are the most suitable to favor cell growing, they contain important domains that send signals to cells to favour their development, but at the same time these polymer could cause antigenicity [10]. The most common natural polymers are proteins particurarly those extracted from extracellular matrix, i.e collagen and glycosaminoglycan, or polypeptides, polysaccharides (chitosan, hyaluronic acid and alginate). Synthetic polymers can be modulated in many ways such as mechanical properties (strength and modules), degradation rate, molecular weight and chemical modification. In addition, they can be manufactured in a large scale. The most

popular biodegradable synthetic polymers include poly (α-hydroxy acids) such as poly (glycolic acid) PGA , poly (D,L-lactic acid)PLA, and their copolymers poly (lactic-co-glycolic acid) PLGA, poly(ε-caprolactone), poly(propylene fumarate), poly(dioxanone), poly orthoesters, polycarbonates. Poly (ethylene glycol) PEG is a linear polyether that is used extensively in biomedical applications due to its hydrophilic and highly biocompatible properties, and at low molecular weight can be safely excreted by metabolism in body. Some products, such as Hyaff®-11 (FIDIA Advanced Biopolymers, Italy) are already commercialized.

1.2 Bone

1.2.1 Bone repair

Bone possesses the intrinsic capacity for regeneration as part of the repair process in response to injury, as well as during skeletal development or continuous remodelling throughout adult life. Bone regeneration is comprised of a well-orchestrated series of biological events of bone induction and conduction, involving a number of cell types and intracellular and extracellular molecular-signalling pathways, with a definable temporal and spatial sequence, in an effort to optimise skeletal repair and restore skeletal function [11]. In the clinical setting, the most common form of bone regeneration is fracture healing, during which the pathway of normal fetal skeletogenesis, including intramembranous and endochondral ossification, is recapitulated [12]. Unlike in other tissues, the majority of bone injuries (fractures) heal without the formation of scar tissue, and bone is regenerated with its pre-existing properties largely restored, and with the newly formed bone being eventually indistinguishable from the adjacent uninjured bone [11]. When this natural process do not occur, because of fracture non-unions or large scale traumatic bone injury, surgical intervention is warranted. A surgical approach concerns the use of rigid internal fixation, which is a nonresorbable material and are susceptible to long-term fatigue and fracture. Bone grafting is a commonly performed surgical procedure to augment bone regeneration in a variety of orthopaedic and maxillofacial procedures, with autologous bone being considered as the 'gold standard' bone-grafting material, as it combines all properties re-

quired in a bone-graft material: osteoinduction (bone morphogenetic proteins (BMPs) and other growth factors), osteogenesis (osteoprogenitor cells) and osteoconduction (scaffold) [13]. Furthermore, because it is the patient's own tissue, autologous bone is histocompatible and non-immunogenic, reducing to a minimum the likelihood of immunoreactions and transmission of infections. Nevertheless, harvesting requires an additional surgical procedure, with well documented complications and discomfort for the patient, and has the additional disadvantages of quantity restrictions and substantial costs [14, 15]. An alternative is allogeneic bone grafting, obtained from human cadavers or living donors, which bypasses the problems associated with harvesting and quantity of graft material. There are issues of immunogenicity and rejection reactions, possibility of infection transmission, and cost [16]. Given the shortcomings of autografts and allografts and the large demand for bone grafts, tissue engineering approaches emerged as a potential alternative therapeutic process to treat severely injured patients with minimally invasive techniques. Tissue engineering represents one promising strategy.

1.2.2 Bone tissue engineering

Bone tisse engineering develops graft substitutes formed from a variety of materials (natural and synthetic polymers, ceramics, and composites) that are designed to mimic the three-dimensional characteristics of autograft tissue while also providing the ability to sustain cells seeded onto the construct [17, 18, 19]. In addition to appropriate mechanical properties, the scaffold must also have the right internal micro-architecture with interconnected pores of 200-400 μm diameter (the average size of the human osteon is approximately of 223 μm) [20]. Pore size is known to affect cellular affinity and viability by influencing cellular movement, binding and spreading, intracellular signaling, and transport of nutrients and metabolites [21]. The inorganic phase is represented by ceramics, such as hydroxyapatite (HA) or other calcium phosphate (Ca-P) ceramics (including tricalcium phosphate, TCP) or bioactive glasses (such as Bioglass®). They are known to promote, when implanted, the formation of a bone-like apatite layer on their surfaces. This is considered to be a positive characteristic in terms of bone-bonding behaviour, assuring enhanced fixation of the implant [22, 23, 24].

Even if hydroxyapatite, calcium phosphate and a wide variety of ceramic matrices are appropriate for cell transport as they stimulate their differentiation and bone growth, they are not osteoinductive and they are reabsorbed relatively slowly. Also, there are problems associated with biodegradability, inflammatory and immunological reactions when they are used as carriers of osteoinductive factors. To overcome these drawbacks the inorganic phase is combined with natural or synthetic polymers or polymer precursors, above mentioned, that will allow produce bioactive, inert, biodegradable or injectable composites [25]. Injectable materials (small particles or semi-liquid polymers that can be cross-linked in situ) are preferable for irregular defects reconstruction, while solid materials are more appropriate for large bone defects [26]. These materials can also acellular or celluar. Acellular materials can be solid, absorbable fillers that will disappear with time, or porous scaffold that can be rapidly colonized by cells. Instead, cellular materials are structures in which a cellular component is embedded prior to implantation. Inclusion of growth factors in the scaffolds may be a route for its controlled delivery during the differentiation process. A briefly description of materials used in this thesis will follow in the next section.

1.3 Material selection

1.3.1 Gelatin

Gelatin is widely used in the pharmaceutical industry as well as in the biomedical field: hard and soft capsules, microspheres, sealants for vascular prostheses, wound dressing and adsorbent pad for surgical use are among its most frequent applications. Gelatin is obtained by thermal denaturation or physical and chemical degradation of collagen which involves the breaking of the triple-helix structure. The result is a biodegradable, biocompatible and nonimmunogenic product, suitable for medical applications [27]. At a temperature of about 40°C, gelatin aqueous solutions are in the sol state and form physical thermoreversible gels on cooling. During gelling, the chains undergo a conformational disorder-order transition and tend to recover the collagen triple-helix structure [28]. As a biomaterial, gelatin displays several attractivness: it is a natural polymer which has

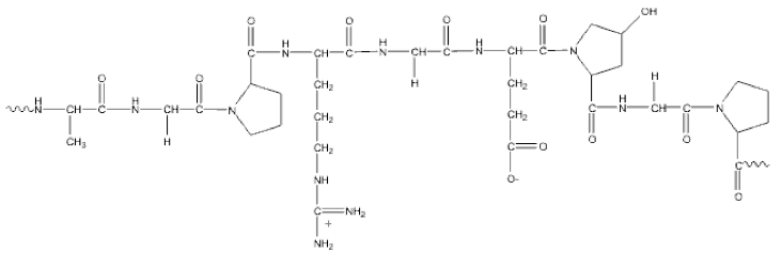

Figure 1.3.1: *Gelatin structural unit.*

not shown antigenity, it is completely resorbable in vivo and its physicochemical properties can be suitably modulated [29, 30].

Commercially there are two processes for the production of gelatine from collagen. In the first method, the *alkali process*, the raw material is treated with a basic suspension to dissolve impurities. It is suitable to destroy certain chemical crosslinkages still present in a more complex collagen e.g. collagen from bovine skin and bone, but this process requires longer time, normally several weeks. The gelatin obtained from this process is referred to as type-B gelatin. The second or *acid* process does not involve a pretreatment, is especially suitable for less fully crosslinked materials such as pig skin collagen. Pig skin collagen is less complex than the collagen found in bovine hides. Acid treatment is faster than alkali treatment and normally requires from 10 to 48 hours. This gelatin is called type-A gelatin. It is important to know by which of these two processes the gelatin was made, since the two types differ in properties. They have different viscosity, gel strength (Bloom index) and different isotonic point. Gelatin obtained is a heterogeneous mixture of single or multi-stranded polypeptides, each with extended left-handed proline helix conformations and containing between 50 - 1000 amino acids. Gelatin contains many glycine (almost 1 in 3 residues, arranged every third residue), proline and 4-hydroxyproline residues. A typical structure is -Ala-Gly-Pro-Arg-Gly-Glu-4Hyp-Gly-Pro- (fig. 1.3.1).

Thanks to the large number of functional side groups it contains, gelatin readily undergoes chemical cross-linking, which is very important for its possible use as a biomaterial. In fact, as collagen based biomaterials are rapidly degraded in vivo, their structure must be reinforced so that they will not significantly alter

in the body for the required period. This is usually achieved through the use of cross-linking agents. Gelatin used in this work is gelatin type A from porcine skin (Sigma Aldrich, Italy).

1.3.2 Collagen

Collagen is the major insoluble fibrous protein in the extracellular matrix and in connective tissue. There are at least 16 types of collagen, but 80%-90% of collagen in the body consists of type I, II and III (figure1.3.2).

Type	Molecule Composition	Structural Features	Representative Tissues
Fibrillar Collagens			
I	$[\alpha1(I)]_2[\alpha2(I)]$	300-nm-long fibrils	Skin, tendon, bone, ligaments, dentin,interstitial tissues
II	$[\alpha1(II)]_3$	300-nm-long fibrils	Cartilage, vitreous humor
III	$[\alpha1(III)]_3$	300-nm-long fibrils; often with type I	Skin, muscle, blood vessels
V	$[\alpha1(V)]_3$	390-nm-long fibrils with globular N-terminal domain; often with type I	Similar to type I; also cell cultures, fetal tissues
Fibril-Associated Collagens			
VI	$[\alpha1(VI)][\alpha2(VI)]$	Lateral association with type I; periodic globular domains	Most interstitial tissues
IX	$[\alpha1(IX)][\alpha2(IX)]$ $[\alpha3(IX)]$	Lateral association with type II; N-terminal globular domain; bound glycosaminoglycan	Cartilage, vitreous humor
Sheet-Forming Collagens			
IV	$[\alpha1(IV)]_2[\alpha2(IV)]$	Two-dimensional network	All basal laminaes

Figure 1.3.2: *Principal types of collagen*

These collagen types are usually packed togheter to form long thin fibrils. While type IV forms a two dimensional reticulum, several other types associate with fibril-type collagens linking them to each other or to other matrix components. At one time it was thought that all collagens were secreted by fibroblasts in connective tissue, but we now know that numerous epithelial cells make certain types of collagens. The first collagen characterized was type I collagen. Its

fundamental structure is a long and thin protein made of three α chains subunits, arranged in a right-handed triple helix. There are at least 30 different types of α chains that may result in theory in 20000 different triple helices, but we know only 19 types. The triple-helical structure of collagen arises from an unusual abundance of three amino acids: glycine, proline, and hydroxyproline. These amino acids make up the characteristic repeating motif Gly-Pro-X, where X can be any amino acid. Each amino acid has a precise function. The side chain of glycine, an H atom, is the only one that can fit into the crowded center of a three-stranded helix. Hydrogen bonds linking the peptide bond NH of a glycine residue with a peptide carbonyl group in an adjacent polypeptide help hold the three chains together. The fixed angle of the C-N peptidyl-proline or peptidyl-hydroxyproline bond enables each polypeptide chain to fold into a helix with a geometry such that three polypeptide chains can twist together to form a three-stranded helix. Many three-stranded type I collagen molecules pack together side-by-side, forming fibrils with a diameter of 50-200 nm. In fibrils, adjacent collagen molecules are displaced from one another by 67 nm, about one-quarter of their length. This staggered array produces a striated effect that can be seen in electron micrographs of stained collagen fibrils; the characteristic pattern of bands is repeated about every 67 nm (figure 1.3.3 on the next page).
Type I collagen fibrils have enormous tensile strength; that is, such collagen can be stretched without being broken. These fibrils, roughly 50 nm in diameter and several micrometers long, are packed side-by-side in parallel bundles, called collagen fibers [31](figure 1.3.4 on page 12). This collagen type has been used in this work, it was extracted from Wistar rat tail [32].
The critical aspect in using collagen gel as a biomaterial, is that its mechanical strength is too small and easily deforms its triple-helix structure into a random coil structure when heated and it dissolves in water. Like gelatin to overcome these problems, chemical crosslinking methods have been used.

1.3.3 Genipin

Genipin has been used in this work as crosslinker, chosen among the most used crosslinkers, on the basis of its chemical features and reduced toxicity. In chemical cross-linking methods, cross-linkers are used to bond functional groups of amino

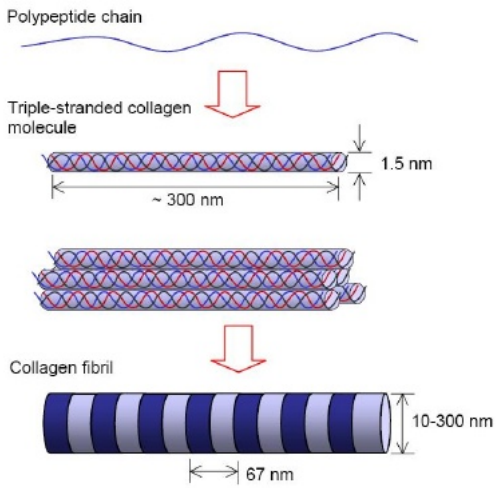

Figure 1.3.3: *Schematic diagram of Type I collagen fibril structure.*

acids. Commonly used chemical cross-linkers include formaldehyde, glutaraldehyde, polyepoxy compounds, tannic acid, dimethyl suberimidate, carbodiimides and acyl azide. However, these synthetic cross-linking reagents were relatively highly cytotoxic, impairing the biocompatibility of bioprostheses [33, 34]. This is the reason for the increasing demand for a cross-linking reagent that can form stable and biocompatible cross-linked products, without causing problems of cytotoxicity. Genipin showed to be a low-toxic and naturally occurring cross-linking agent [35, 36, 37]. It was about 10000 times less cytotoxic than glutaraldehyde [35], and it can form stable cross-linked products with resistance against enzymatic degradation that is comparable to that of glutaraldehyde-fixed tissue [38]. Genipin and its related iridoid glucosides, are extracted from the fruits of Gardenia jasminoides Ellis. The fruit is an oriental folk medicine which has been included in traditional formulations. Its folkloric use was for the treatment of inflammation, jaundice, headache, edema, fever, hepatic disorders and hypertension, and its pigments were used as food colorants in oriental countries. The pharmacological actions of the whole fruit, such as protective activity against oxidative damage, cytotoxic effect, antiinflammatory activity and fibrolytic activity have already been elucidated [39]. Among the drug extracted form the dried fruit

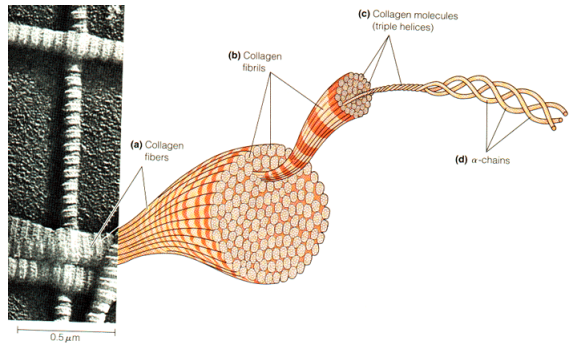

Figure 1.3.4: *The structure of collagen, from the a chains to the fiber.*

of gardenia, geniposide is one of the major iridoid glycosides and is hydrolyzed to the aglycone genipin (figure 1.3.5).

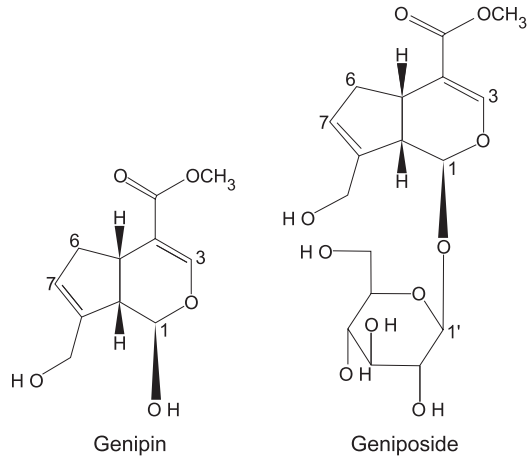

Figure 1.3.5: *The chemical structures of genipin and geniposide.*

The same Genipin has been shown to inhibit hepatocyte apoptosis induced by transforming growth factor β1, via the interference with mitochondrial permeability transition [40], and to protect hippocampal neurons from Alzheimer's amyloid β protein toxicity [41]. Genipin was found to possess a significant an-

tilipoperoxidative, antiinflammatory, and potent antiangiogenic activities. The latter activity could let genipin be used as adjuvant or combination chemotherapy for the treatment of cancer [42]. The great advantage of genipin is to be not only a crosslinker, but it is able also to reduce the inflammatory response of the engineered tissue upon implantation [43].

As far as genipin crossliking activity, it reacts with primary amino groups of amino acid or proteins to form dark blue pigments. The mechanism of the reaction of amino acids or proteins with genipin will be explained later.

1.3.4 Hydroxyapatite

Bone is a complex material composed of nanocrystals of a basic calcium phosphate deposited within an organic matrix. The inorganic phase of bone is assimilated to synthetic hydroxyapatite (HA), $Ca_{10}(PO_4)_6(OH)_2$. HA has the ability to induce mesenchymal stem cells differentiation towards osteoblasts [44], whereas nanosized HA has been found to improve osteoconductivity due to its similarity with morphology of bone minerals [45]. When implanted *in vivo*, this material is non-toxic, antigenically inactive, do not induce cancer and bond directly to bone without any intervening connective tissue layer. Recent reports on ectopic bone formation (osteoinduction or material-induced osteogenesis) of calcium phosphate biomaterials showed that osteoinduction might be an intrinsic property of calcium phosphate biomaterials [46, 47]. The addition of HA in the gelatin/HA composites has been found to improve the mechanical properties of scaffolds and the activity and viability of rat osteoprogenitor cells cultured on them [48].

2 Genipin reaction

Abstract

In this chapter genipin crosslinking reaction will be describe, to optimize the experimental protocol for scaffold manifacturing. Particularly, kinetic constant and diffusion constant have been studied, while mechanism reaction has been already described in literature. Finally, to establish the degree of crosslinking, fluorescamine assay ha been performed.

2.1 Introduction

2.1.1 Mechanism reaction

Previous studies [35, 49] have demonstrated that genipin reacts with materials containing primary amine groups, such as chitosan, gelatin and some peptides and polypeptides, to form covalently crosslinked networks. It is believed that the crosslinks are formed via a series of reactions involving different sites on the genipin molecule ending with a radical polymerization responsible of the blue product. Thanks to radical reactions genipin is able to establish long-range intermolecular crosslinks, besides intramolecular and short-range intermolecular crosslinks respect to the other crosslinkers e.g. 1-ethyl-3-(3-dimethyl aminopropyl)-carbo-diimide (EDC) and N-hydroxysuccinimide (NHS), or glu-

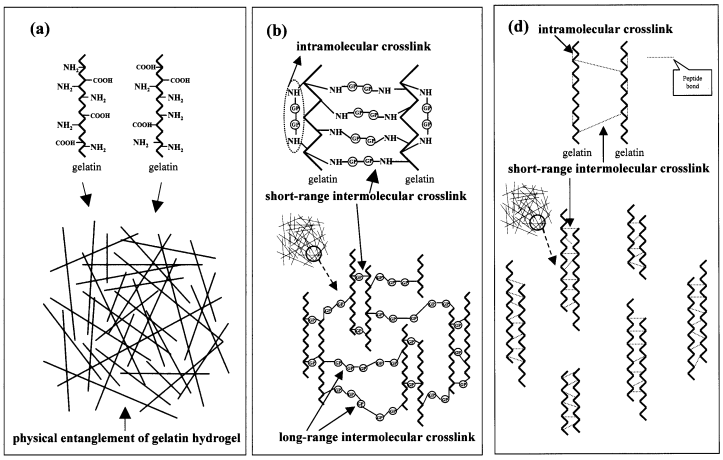

Figure 2.1.1: *Crosslinking structures presumed for (a) a fresh gelatin hydrogel (a gelatin hydrogel without crosslinking), (b) a GP-crosslinked gelatin hydrogel, (c) an EDC/NHS-crosslinked gelatin hydrogel.*

taraldehyde [50](fig.2.1.1).

The polymerization reaction involves a S_N2 nucleophilic substitution reaction that involves the replacement of the ester group on the genipin molecule by a secondary amide linkage. This reaction is slower than the other reaction which must have already formed by the time that the ester substitution occurred. The reaction scheme begins with an initial nucleophilic attack of the genipin C3 carbon atom from a primary amine group to form an intermediate aldehyde group. Opening of the dihydropyran ring is then followed by attack on the resulting aldehyde group by the secondary amine formed in the first step of the reaction. A heterocyclic compound of genipin linked to the residues containing primary amine groups in gelatin is thereby formed (fig.2.1.2). The formation of blue pigments suggests that, in addition to these reactions, other more complex reactions occurred. Previous studies of the blue pigments obtained in the reaction of genipin with amino acids [51] found that they were formed from the oxygen radical-induced polymerization of genipin and dehydrogenation of intermediate compounds, following the ring-opening reaction because of attack of genipin by a primary amine group. The polymerization reactions are induced by the presence

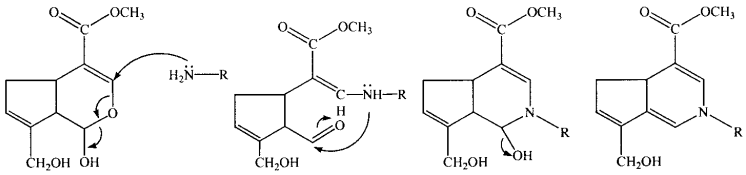

Figure 2.1.2: *The fastest crosslinking reaction involving genipin.*

of oxygen radicals because the blue coloration was initially more pronounced at the interface of the gelled samples and gradually moved down through the sample with time. When the radical reaction starts, genipin molecules react with one (a dimery) or more genipin molecules before crosslinking with amino group-containing compounds, so we can explain the long-range intermolecular crosslinking (fig.2.1.1). Moreover Butler et al. [52] showed that the radical reaction occurs only after that one of the previous reactions described take place. No blue pigments formed when genipin was mixed with acetyl-glucosamine because it was unable to initiate either of the crosslinking reactions.

The crosslinking genipin reaction is strongly pH dependent. At a high basic pH, the polymerization of genipin molecules is favoured to link protein chains distant from each other, but the final product shows a low crosslinking degree, a high swelling and high enzymatic hydrolysis rate. While at acid or neutral pH, genipin can for maximum a tetramer, so shorter links, but with a lower swelling and enzymatic hydrolysis [53].

2.1.2 Reaction rate constant and order reaction

It is important to know when the reaction between gelatin/collagen and genipin can be considered ended. On the contrary with the other crosslinkers, genipin reaction is not so fast, so in this work the reaction has been studied over a period of 48 hours. Rate equation for a chemical reaction is an equation that links the reaction rate with concentrations or pressures of reactants and constant parameters (normally rate coefficients and partial reaction order). For a reaction aA+bB→pP

$$v = k\,[A]^m\,[B]^n$$

Where k is the reaction rate coefficients that quantifies the speed of a chemical reaction, it depends on temperature not on reagent or on product concentration. While m and n are not the stoichiometric coefficients of the balanced equation, they must be determined experimentally, and they are the order of the reaction with respect to reagent or product while the sum of m and n is the overall order of reaction. Reactions may commonly be zero order, first order or second order. A reaction is zero order when changing the concentration of the reactant has no effect on the reaction rate. A reaction that is first order has its rate doubled when the concentration of that reactant is doubled.

$$v = k\,[A]$$

Where doubling the concentration of a reactant results in a quadrupling (x4) of the rate, the reaction is second order.

$$v = k\,[A]^2$$

The order of reaction with respect can be establish from a concentration against time graph. However, it can sometimes be difficult to decide if a reaction is first-order or second-order from the concentration-time graph. A rate-concentration graph quickly reveals the order with respect to a reactant (fig. 2.1.3).

Reactions can also have an undefined reaction order with respect to a reactant. The common method used to determine the rate equation is the *isolation method*. The concentration of one of the reactants remains constant, because it is in great excess with respect to the other reactants, so its concentration can be included in the rate constant, obtaining a pseudo constant. If B is the reactant whose concentration is constant then

$$v = k\,[A]^m\,[B]^n = k'\,[A]^m\,.$$

This is the treatment to obtain an integrated rate equation much easier.

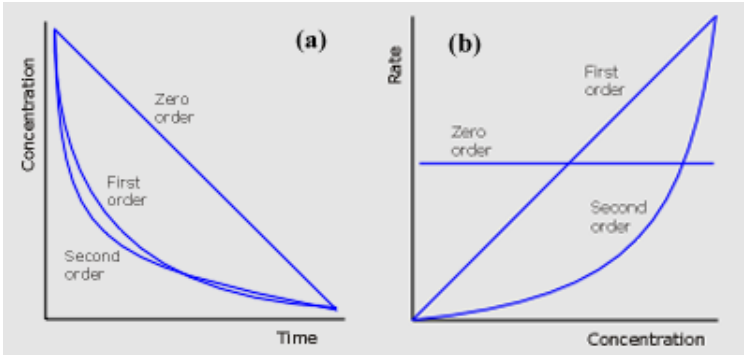

Figure 2.1.3: *(a) Concentration-time graph and (b) rate-concentration graph to evaluate order reaction.*

2.1.3 Diffusion coefficient

Diffusion, is the thermal motion of all liquid or gas particles at temperatures above absolute zero. Diffusion explains the net flux of molecules from a region of higher concentration to one of lower concentration, but it is important to note that diffusion also occurs when there is no concentration gradient. Diffusive equilibrium is reached when the concentrations of the diffusing substance in the two compartments becomes equal. Molecular diffusion is typically described mathematically using Fick's laws of diffusion.

$$J = -D\frac{dC}{dx} \tag{2.1.1}$$

Equation 2.1.1, is the first Fick's law that relates the diffusive flux J to the concentration by postulating that the flux goes from regions of high concentration to regions of low concentration with a magnitude that is proportional to the concentration gradient. Flux doesn't change with time, the system is in the steady state. It is important to determine rate of genipin diffusion through gelatin, that is *diffusion coefficient*, but it is also hard because genipin diffusion involves also a chemical reaction with gelatin. Free diffusion through a membrane is linked to flux definition and Teorell equation. The flux in free diffusion can be written in a form proposed by Teorell (eq.2.1.2)

$$J_s = \eta_s \cdot C_s \cdot \nabla \mu_s \tag{2.1.2}$$

where $J_s$is the flux, that is the numbers of mols of solute crossing one square meter of membrane per second, and it proportional to the product of $\eta_s$that is the solute mobility, to C_s that is the solute concentration, and $\nabla \mu_s$ is the driving force of the solute. The choice of a proper driving force is dictated by thermodynamic considerations by analogy with electrical phenomena. When the chemical potential of the solute is the same in the two phases bounding the membrane, the solute is in equilibrium, and its flux across the membrane is zero. An analogous situation occurs in electrical circuits; when there is no electrical potential difference, there is no current flow. When the electrical potentials at two points are different, the potential gradient defines a field, and charged particles move in response to it. The force acting on the charges is the negative of the electrical potential gradient. The analogous driving force for solute flux is the negative of the chemical potential gradient -$\nabla \mu_s$. Diffusion coefficient D is linked with its mobility η by the equation 2.1.3:

$$D = \eta \cdot R \cdot T \tag{2.1.3}$$

where $R = 8.3144 \cdot {}^{J}/_{(mol \cdot K)}$ is the ideal gas constant, T is the absolute temperature. Considering Stokes-Einstein equation for diffusion of spherical particles through liquid (eq2.1.4):

$$D = \frac{k_B \cdot T}{6\pi \cdot \nu_f \cdot r} \tag{2.1.4}$$

where $k_B = 1.381 \cdot 10^{-23} {}^{J}/_{K}$ is the Boltzmann constant, ν_f is the fluid viscosity, and r is the particle radius, D depends on the solute dimension particularly on its radius. Decreasing particle radius, D will increase so the particle transport would be easier. So using a material with a similar viscosity to gelatin, but unreactive with genipin could be a method to obtain a real diffusion coefficient of genipin. The material choosen was agarose.

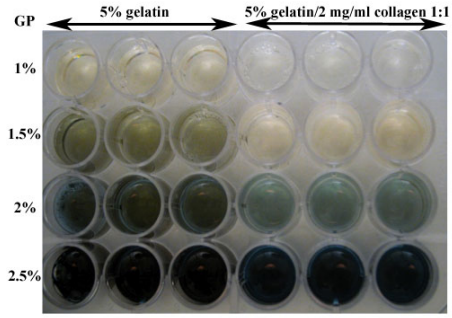

Figure 2.2.1: *Gelatin and gelatin/collagen samples crosslinked with genipin at different concentrations.*

2.2 Experimental section

2.2.1 Sample preparation to evaluate reaction rate constant

The rate constant has been studied for the genipin crosslinking reaction with gelatin alone, and gelatin mixed with collagen. Gelatin type A from porcine skin was purchased from Sigma-Aldrich (Italy). 5% w/v gelatin solution was obtained dissolving gelatin in phosphate buffered saline (PBS), heating and mixing it to 70°C on a stirrer for 1h till the solute was totally dissolved. Collagen type I was extracted from rat tail [32] with a 4 mg/ml concentration. Genipin (98% by HPLC) was purchased from Challenge Bioproducts Co., Ltd (CBC, Taiwan).

A series of samples were prepared mixing 5% w/v gelatin with genipin a different concentration: 2.5%, 2.0%, 1.5%, 1.0%, 0.5%, 0.25%, 0.125% e 0.06% w/w of the gelatin solution weight. The solutions were stirred to favour genipin dissolution and let to crosslink in a 24 multiwell plate once at room temperature and once at 37°C. Other samples were prepared mixing 5% gelatin and 2 mg/ml collagen solutions in a 1:1 weight ratio (i.e 1g of gelatin with 1g of collagen) and were crosslinked with the same genipin concentration as above described at room temperature and at 37°C (fig.2.2.1).

2.2.2 Image elaboration

To evaluate the rate reaction, the blue pigment formation was considered as an index of crosslinking progress. The reaction was followed for 48 hours and picture were taken at established time. Wells from pictures were imported as RGB matrices in Matlab. The blue component of each matrix, based on the media value, was extracted after elaboration. Values of the blue intensity were plotted against time and then they were fitted to obtain the progress of crosslinking reaction at different genipin concentration.

2.2.3 Diffusion device

The diffusion device is composed of two adjacent sub-chambers separated by thin removable Teflon divider (S) which contains a thin membrane of gelatin or agarose, as shown in figure2.2.2. Agarose for routine use was purchased from Sigma-Aldrich with a gelling point between 34.5°C and 37.5°C. A 1% w/v agarose solution was prepared in boiling deionized water and allowed to solidify in the divider hole for membrane. The same experimental setting was followed for gelatin membrane prepared with a 5% w/v gelatin solution. The large sub-

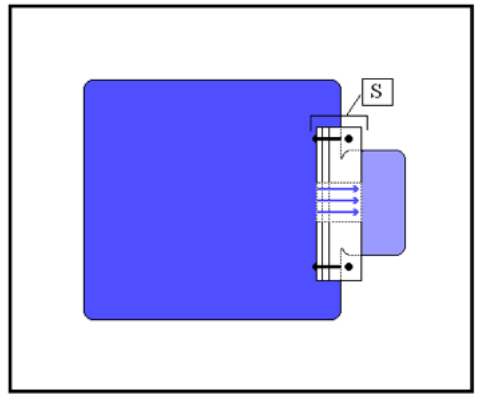

Figure 2.2.2: *Diffusion device.*

chamber is the liquid chamber containing a 0.5% or 0.25% w/v genipin solution in 100 ml of PBS, and the small sub-chamber (diffusion chamber) contains 10 ml

of PBS solution. The sub-chamber is 10 cm x 10 cm and 1 cm in height, while diffusion sub-chamber is 5 cm x 2 cm and 1 cm in height. The divider is composed of three parts as shown in the figure 2.2.3. The first part (A in the figure), has

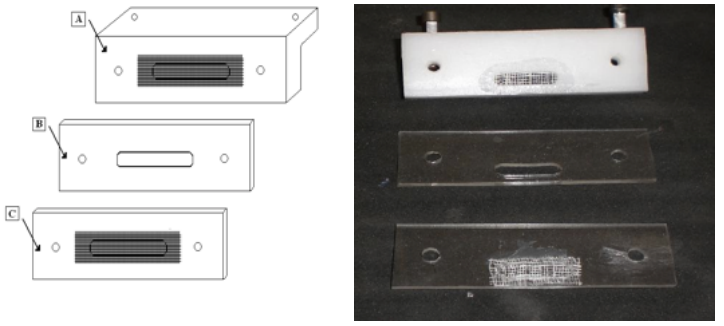

Figure 2.2.3: *Divider composition.*

a central hole with a surface of 1 cm^2. The second part (B in the figure) is a thin silicone film, thickness 1 mm, which support membrane and it is put on the first part A. Finally the third part (C in the figure), is a plexiglass skin put on the previous two parts to hold them. On A an C, a gauze with big mesh to not interfere in the measure, is glued in order to confine membrane in the divider. Thanks to the design of the device some remarks can be made: the ratio 1:10 between volume solutions let the steady state reach quickly; osmotic pressure can be considered in inverse relation to volume, so it has a low value if the solution with genipin is in the bigger chamber and diffusion in the smaller chamber is easier. Samples were collected from the diffusion chamber at established time at room temperature, and genipin concentration was evaluated using FLUOstar Omega spectrofluorimeter (BMG Labtech, Ortenberg Germany) at 244 nm.

2.2.4 Fluorescamine assay

Fluorescamine assay was performed for the quantification of amine groups unreacted (μg/ml) at the end of reaction in order to evaluate the crosslinking degree. The Fluorescamine protein dye is a fluorescent stain for quantitating minute amounts of protein and peptides in solution. Fluorescamine is a spiro compound

that is not fluorescent itself, but reacts with primary amines to form highly fluorescent products when activated with UV light (365nm), and with an emission wavelength of approximately 470nm. The fluorescence of a solution containing protein or other substance with amino groups, plus fluorescamine is proportional to the quantity of free amine groups present. It hence has been used as a reagent for the detection of amines and peptides. 1-100 µg of protein and dowm 10 pg protein can be detected[54]. Samples tested were: 5% gelatin+2 mg/ml collagen in a 1:1 weght ratio crosslinked with different genipin concentration 0.1%, 0.2%, 0.3%, 0.4% w/w. After a casting of 2 days they were freeze-dried for 12 hours. A fresh stock of 3 mg/ml Fluorescamine solution (Sigma-Aldrich, Italy) was preparing dissolving it in DMSO. Stock solution was added to about 5 mg of sample and allow the reaction to incubate at room temperature for 30 minutes. Fluorescence was recorded with FLUOstar Omega spectrofluorimeter (BMG Labtech, Ortenberg Germany) using BSA (bovine serum albumin) at various known concentrations as standard.

2.3 Results

2.3.1 Reaction rate constant

Assuming genipin crosslinking reaction as a first order reaction, and that it occured in one stage, the general chemical equation is eq.2.3.1:

$$A + B \rightarrow P \tag{2.3.1}$$

its rate equation is:

$$v = k\,[A]^m\,[B]^n$$

supposing that B was the reactant in excess respect to A, it can be considered constant and B can be include in the k value, so $k' = k\,[B]^n$ obtaining:

$$v = k'\,[A]^m$$

where, as supposed to be a first order reaction m=1 and

$$v = k' [A] .$$

Instant rate equation was

$$v = -\frac{d[A]}{dt} = k' [A]$$

multiplying both members by $\frac{dt}{[A]}$ and integrating:

$$\int_{[A_0]}^{[A]} \frac{d[A]}{[A]} = \int_0^t -k' dt$$

solving

$$[A] = [A_0] e^{-k't}.$$

The equation including P concentration was obtained from previous one

$$[P] = [A_0] \left(1 - e^{-k't}\right). \tag{2.3.2}$$

In this case, P represents the polymer formation after genipin reaction which was blue and its variation can be considered an index of the progress of reaction. Data obtained from image elaboration were fitted with an equation similar to equation 2.3.2:

$$y = (1 - e^{-bx})c + d \tag{2.3.3}$$

where b is a time constant so it is the rate reaction constant; c is the final blue intensity obtained from image elaboration, chemically the product concentration when reaction ended; d is the initial amount of polymer formed, first blue value. For a first group of gelatin/collagen samples at different genipin concentration, figure2.3.1, experimental data are showed with standard deviation together with the curves obtained from equation 2.3.3 after Matlab elaboration.

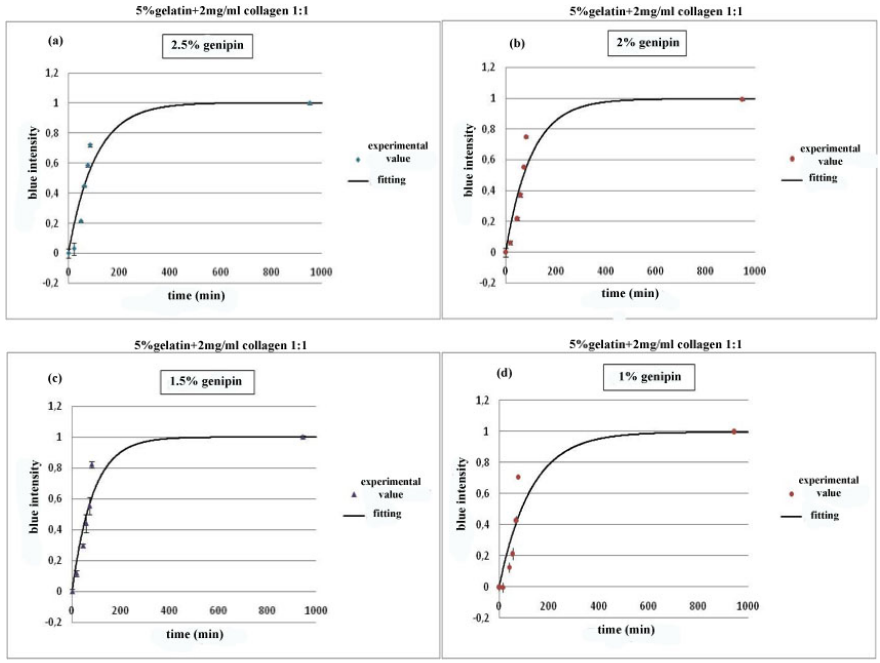

Figure 2.3.1: *Blue intensity against time as expression of rate reaction, for gelatin collagen samples at different genipin concentration (a)2.5%, (b)2%, (c)1.5%, (d)1% w/w.*

While coefficient obtained from equation2.3.3, that best fit experimental data, are displayed in table 2.1.

	2.5%	2%	1.5%	1%	average value	standard deviation
b	0.009444	0.009702	0.00877	0.007814	0.0089	0.0008
c	260.5	259	260.1	258.7	259.575	0.00084
d	3.65E-06	2.55E-06	1.73E-06	3.38E-09	1.98234E-06	0.86168

Table 2.1: *Coefficients from Matlab elaboration for gelatin collagen and high genipin concentration.*

The rate constant reaction b, is expressed in min^{-1} with an average value of

0.0089 min^{-1} or $1.48 \cdot 10^{-3}$ s^{-1}. At lower genipin concentrations, b showed values quite different from previous ones, so they were grouped a part (fig.2.3.2, and table2.2). Coefficients for 0.5% genipin reaction were excluded from the average

	0.25%	0.125%	0.006%	average value	standard deviation
b	0.004146	0.003075	0.002784	0.0033	0.0007
c	4.31E-01	4.30E-01	4.85E-01	4.49E-01	0.031
d	0.5493	0.5509	0.5162	0.5388	0.020

Table 2.2: *Coefficients from Matlab elaboration for gelatin collagen and low genipin concentration.*

value of table2.2, because they were too different respect to the others b=0.13 min^{-1}. The average value b is $3.3 \cdot 10^{-3} min^{-1}$. Blue intensity data from Matlab image elaboration for 5% gelatin and genipin at different concentrations, were fitted with the same equation2.3.3 table 2.3 , and plotted against time fig.2.3.3.

	2.50%	2%	1.50%	1%	average value	standard deviation
b	0.01195	0.01216	0.01169	0.01086	0.0117	0.0006
c	261.5	260.7	260.9	260.1	260.8	0.5774
d	1.92E-07	4.25E-07	1.49E-06	4.67E-07	6.44E-07	5.79E-07

Table 2.3: *Coefficients from Matlab elaboration for 5% gelatin and high genipin concentration*

For this set of experiments the average value b=$1.17 \cdot 10^{-2}$ min^{-1}, or $1.95 \cdot 10^{-4}$ s^{-1}. The last group of gelatin samples with lower gp concentration showed the following graphs fig.2.3.4 and coefficients in table 2.4.

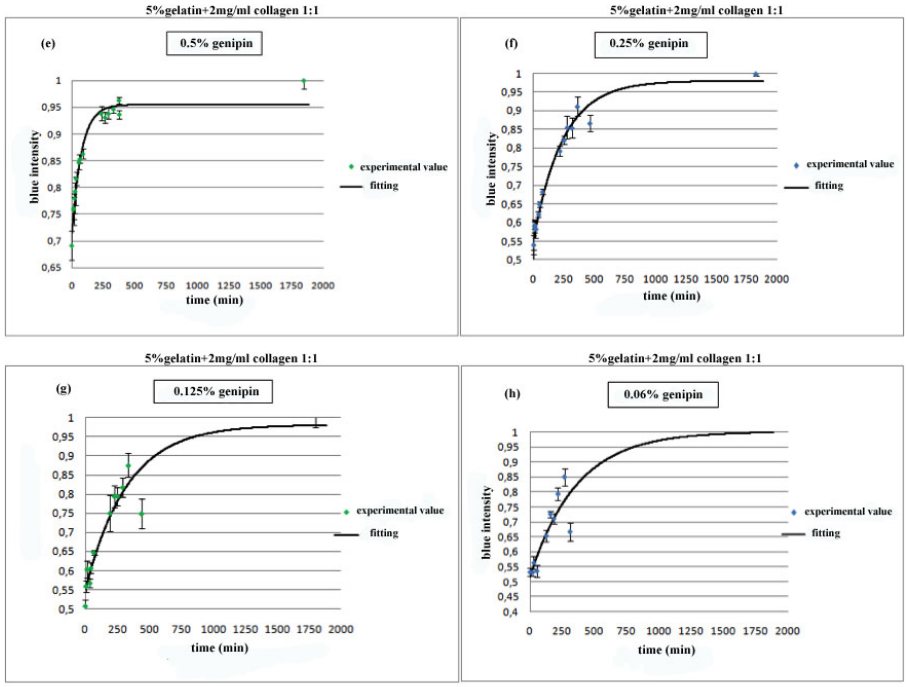

Figure 2.3.2: *Blue intensity against time as expression of rate reaction, for gelatin collagen samples at lower genipin concentration (e)0.5%, (f)0.25%, (g)0.125%, (h)0.06%w/w.*

	0.5%	0.25%	0.125%	0.06%	average value	standard deviation
b	0.01303	0.0129	0.009	0.009592	0.0111	0.0021
c	0.1379	0.3492	0.4189	0.3045	0.3026	0.1195
d	0.8618	0.6427	0.5435	0.5124	0.6401	0.1579

Table 2.4: *Coefficients from Matlab elaboration for 5% gelatin and low genipin concentration*

Average b value is $1.85 \cdot 10^{-4}$ s^{-1} . In table 2.4 c standard deviation is high it is because c decays when genipin concentration decreases.

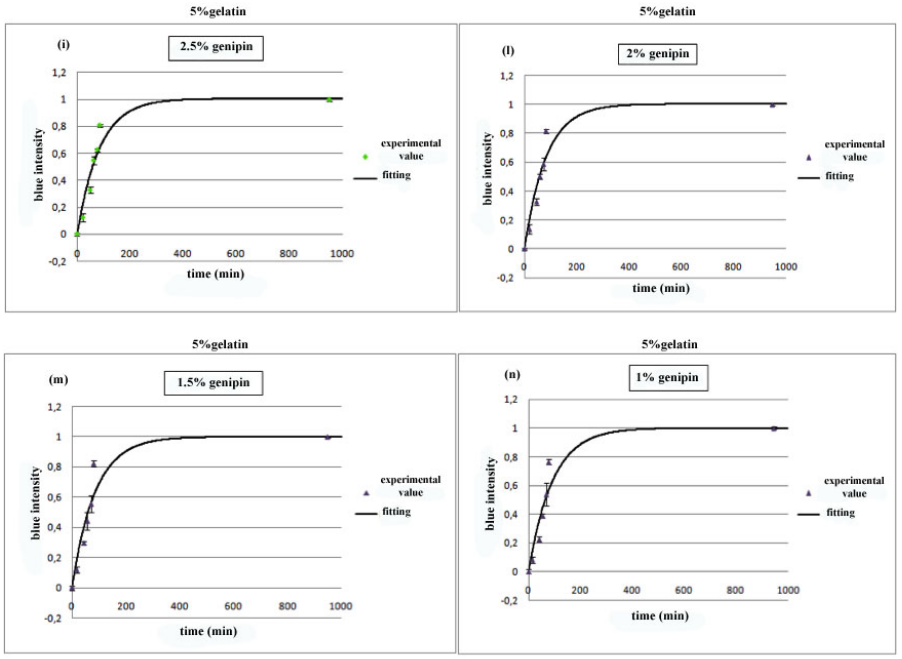

Figure 2.3.3: *Blue intensity against time as expression of rate reaction, for 5% gelatin samples at different genipin concentration (i)2.5%, (l)2%, (m)1.5%, (n)1% w/w.*

2.3.2 Static and dynamic diffusion coefficient

According to the structure of diffusion device (fig.2.2.2), we nominated with D the coefficient diffusion, V_1 the bigger chamber volume and $C_1$the concentration of genipin solution in this chamber, while $V_2$was the smaller chamber volume (diffusion chamber) and $C_2$the concentration of respective genipin solution, L membrane thickness and A its area. The system followed the first Fick's law (eq.2.1.1) in fact it was in a steady state, flux was considered constant within membrane because it was very thin. The number of particles N which pass through a unit area in a unit of time, or flux was expressed as:

$$N = -D\frac{dC}{dx} = \frac{D}{L}\left(C_1 - C_2\right). \tag{2.3.4}$$

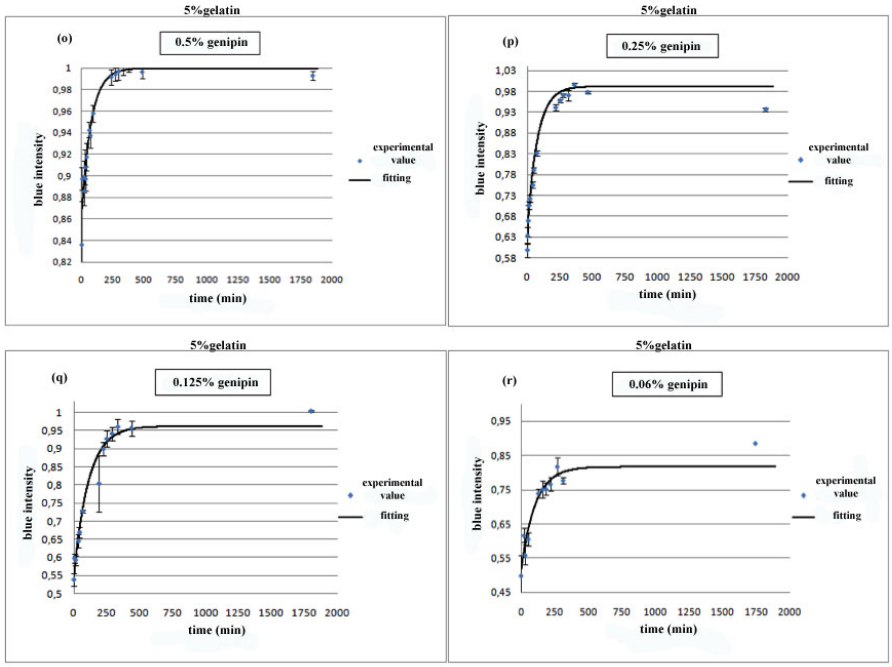

Figure 2.3.4: *Blue intensity against time as expression of rate reaction, for 5% gelatin samples at different genipin concentration (o)0.5%, (p)0.25%, (q)0.125%, (r)0.06% w/w.*

Molecular number was constant in the system so:

$$V_1C_1 + V_2C_2 + V_mC_m = constant \tag{2.3.5}$$

where $V_m$was the membrane volume and $C_m$the genipin concentration within itself. Derivatives of members of eq.2.3.5 was zero:

$$d(V_1C_1) + d(V_2C_2) + d(V_mC_m) = 0. \tag{2.3.6}$$

Membrane thickness was so small respect to V_1 and V_2 that we assumed :

$$V_1dC_1 = -V_2dC_2 \tag{2.3.7}$$

integrating equation 2.3.7:

$$\int_{C_{11}}^{C_{10}} V_1 \cdot dC_1 = -\int_0^{C_2} V_2 \cdot dC_2 \tag{2.3.8}$$

where C_{10} was the starting concentration of genipin solution and C_{11} the final concentration in the bigger chamber. Concentration in the diffusion chamber when experiments started was zero, while final concentration was C_2. Solving equation 2.3.8:

$$V_1 C_{11} - V_1 C_{10} = -V_2 C_2 \tag{2.3.9}$$

and remembering equation 2.3.4

$$J \cdot A = \frac{D-A}{L} \cdot (C_1 - C_2) = -V_1 \cdot \frac{dC_1}{dt} = V_2 \cdot \frac{dC_2}{dt} \tag{2.3.10}$$

we obtained molecular number flowing from V_1 for second or molecules coming in V_2 for second. From equation 2.3.9 this equation was obtained:

$$C_{11} = \frac{V_1 \cdot C_{10} - V_2 \cdot C_2}{V_1} \tag{2.3.11}$$

and replacing it in equation 2.3.10:

$$\frac{D \cdot A}{L} \cdot \left(\frac{V_1 \cdot C_{10} - V_2 \cdot C_2}{V_1} - C_2 \right) = V2 \cdot \frac{dC_2}{dt}; \tag{2.3.12}$$

$$\frac{V_1 C_{10} - (V_1 + V_2)}{V_1 V_2} \frac{DA}{L} dt = dC_2;$$

$$\frac{D \cdot A}{L} \cdot \frac{1}{V_1 \cdot V_2} \cdot dt = \frac{1}{V_1 C_{10} - (V_1 + V_2) \cdot C_2} \cdot dC_2 \tag{2.3.13}$$

integrating eq.2.3.13:

$$\int_0^t \frac{DA}{L} \frac{1}{V_1 V_2} dt = \int_0^{C_2} \frac{1}{V_1 C_{10} - (V_1 + V_2) \cdot C_2} \cdot dC_2; \tag{2.3.14}$$

$$\frac{D \cdot A}{L} \cdot \frac{1}{V_1 V_2} \cdot t = \frac{1}{-(V_1 + V_2)} \cdot [ln(V_1 \cdot C_{10} - (V_1 + V_2) \cdot C_2) - ln(V_1 \cdot C_{10})];$$

$$-\frac{DA}{L}\frac{V_1 + V_2}{V_1 V_2} t = ln\left(\frac{V_1 C_{10} - (V_1 + V_2) C_2}{V_1 C_{10}}\right);$$

$$e^{\frac{D A \cdot V_1 + V_2}{L \cdot V_1 V_2} \cdot t} = 1 - \frac{(V_1 + V_2) \cdot C_2}{V_1 C_{10}} \tag{2.3.15}$$

from eq.2.3.15 C_2 was deduced and then implemented in Matlab:

$$C_2 = \frac{V_1 C_{10}}{V_1 + V_2} \alpha \cdot \left(1 - e^{\frac{D A \cdot V_1 + V_2}{L \cdot V_1 V_2} \cdot t}\right). \tag{2.3.16}$$

α coefficient was linked to the genipin molecules adsorption on gelatin and agarose membrane. This phenomenon limits molecules motility through membrane, and coefficient diffusion decreases with time. D in equation 2.3.16 was obtained from fitting equation. C_{10}, the starting concentration in the big chamber was 5000 µg/ml or 2500 µg/ml. Genipin concentrations in diffusion chamber for agarose and gelatin membrane, collected from spectrofluorimeter were plotted on a graph versus time fig.2.3.5 and 2.3.6 and fitted with a simplified equation deduced from equation 2.3.16:

$$y = \alpha \cdot C_e \left(1 - e^{-bx}\right) \tag{2.3.17}$$

where C_e is the equilibrium value to which the system tends, b is the same exponent of equation 2.3.16, x is time and α will be explain later.

$$b = \frac{A}{L}\frac{V_1 + V_2}{V_1 V_2} D;$$

$$D = \frac{V_1 V_2 A}{V_1 + V_2} L b.$$

Replacing the experimental volume values and membrane thickness L:

$$D = 4.5 \cdot 10^{-6} b. \tag{2.3.18}$$

From equation 2.3.18, replacing b values derived from Matlab (table 2.5 on the facing page and 2.6 on the next page), we had coefficient diffusion D for

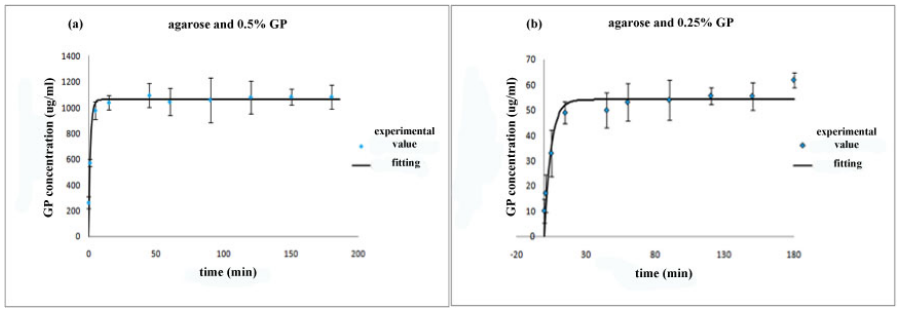

Figure 2.3.5: *Genipin concentrations in diffusion chambers through 1% w/v agarose membrane versus time and fitting curve; (a) 0.5% w/v genipin concentration and (b) 0.25% w/v genipin concentration in the bigger chamber.*

agarose, *static coefficient*, and for gelatin, *dynamic coefficient*.

	Agarose membrane	
	0.25% GP	0.5% GP
α	0.0267 (0.02527, 0.02814)	0.2361 (0.2179, 0.2542)
b	0.8946 (0.5275, 1.262)	0.7442 (0.2947, 1.194)

Table 2.5: *Coefficients from Matlab elaboration with its confidence interval for genipin diffusion through agarose.*

	Gelatin membrane	
	0.25% GP	0.5% GP
α	0.02165 (0.01972, 0.02357)	0.1994 (0.1813, 0.2175)
b	0.2134 (0.09241, 0.3343)	0.1892 (0.08195, 0.2965)

Table 2.6: *Coefficients from Matlab elaboration with its confidence interval for genipin diffusion through gelatin.*

Static coefficient, referred to agarose, considers only diffusive forces and its calculated value from equation 2.3.18 and b Matlab coefficient was $3.35 \cdot 10^{-6} m^2/s$

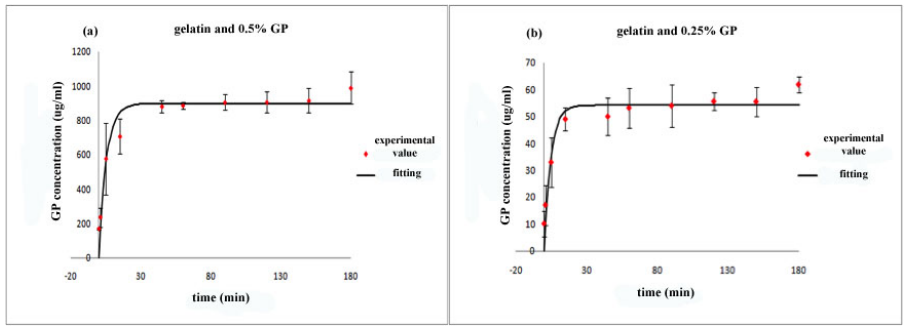

Figure 2.3.6: *Genipin concentrations in diffusion chambers through 5% w/v gelatin membrane versus time and fitting curve; (a) 0.5% w/v genipin concentration and (b) 0.25% w/v genipin concentration in the bigger chamber.*

for 0.5% w/v genipin solution and it was $4.02 \cdot 10^{-6}$ m^2/s for 0.25% w/v genipin solution. *Dymanic coefficient*, referred to gelatin membrane, involves the crosslinking reaction between amino groups of gelatin and genipin and its calculated value was $8.5 \cdot 10^{-7}$ m^2/s for 0.5% w/v genipin solution and it was $3.2 \cdot 10^{-7}$ m^2/s.

2.3.3 Fluorescamine assay

From calibration BSA curve, we obtained the free amino groups content for μg/ml of gelatin-collagen sample, shown in figure 2.3.7. The last sample with 0.4% w/w

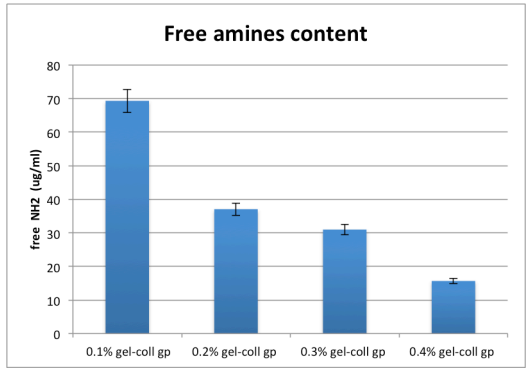

Figure 2.3.7: *Free amino groups content at different GP concentrations.*

genipin content, resulted fewer in weight respect to other samples after freeze dryed, so it is not so a relialable value. Increasing genipin content, free amino groups decreases, it was evident going from 0.1% to 0.2% GP concentrations while there was not so difference between 0.2% and 0.3% samples. The crosslinking reaction with 0.2% GP content can be considered almost ended.

2.4 Conclusions

Genipin crosslinking was characterized regard to rate constant, diffusion coefficient and free amino content at the end of reaction. Kinetic data suggested that after 48 hours, reaction at different GP concentrations can be considered completed, a plateau was reached. We could distinguish two groups for gelatin/collagen samples with different rate constant on the basis of GP concentrations: gelatin/ collagen samples with GP concentrations 2.5%, 2%, 1.5% and 1% showed a higher rate constant respect to lower GP concentrations 0.5%, 0.25%, 0.125% and 0.06%. While for gelatin samples rate constant was almost similar for every GP concentrations. An explanation could be find considering the different molecular organization between gelatin and collagen. The first is obtained from the denaturation of the second, so gelatin shows linear chains with well exposed amino groups while collagen mantains its globular structure and amino groups are not so easily reached by genipin. Comparing the static and dynamic coefficient for both 0.5% and 0.25% GP concentrations, the first resulted bigger, it was because there was no chemical reactions involved in the diffusion process, in fact the crosslinking of gelatin membrane could prevent genipin diffusion. From a deep analysis of this process we made some remarks. Diffusion is a slow process and in this case after 3 hours the system didn't reach equilibrium, it was considered a pseudo-equilibrium. Measuring the GP concentration of both chambers at the end of the experiment there was a missing genipin weight. Really it was not a loss but genipin remained trapped in agarose and in gelatin membrane, besides chemical reaction in the latter one. In agarose membrane there was 4.4% of genipin trapped when the starting concentration in the big chamber was 0.25% and 11.8% when concentration was 0.5%, while in gelatin remained 5.7% and 16.8% of genipin starting respectively from 0.25% and 0.5% GP concentration.

These phenomena are strictly linked with diffusion coefficient reduction, and it's difficult to find a mathematical model that could explain perfectly this particular diffusion process. Even if rate constant for 2.5% GP concentration is higher, this concentration revelead toxic for cells and as fluorescamine assay assessed that there was not so difference in crosslinking degree when using 0.3% and 0.2% w/w GP concentration, chosen concentration for preparing samples was 0.2%.

3

Scaffold preparation and mechanical tests

Abstract

This chapter will deal with the optimal protocol to prepare cartilage and bone scaffolds after selection of suited materials and it will deal with their mechanical characterization, GABO and stress strain tests. Scaffold morphology was evaluated by SEM analysis, while a qualitative-quantitative analysis of materials distribution was obtained with SEM+EDX analysis. The caracterization starts with samples with high genipin content 2.5% w/w, thinking that was most important the gelling time, but later this concentration was found to be over the toxic genipin value reported in literature. So the genipin content was decreased till 0.2% w/w and Young's modulus was measured again. Two protocols for bone scaffolds preparation, both involving ultrasound were compared and increasing HA content.

3.1 Introduction

Tissue engineering goal is to design a scaffold with the same physical characteristics of tissue to be replaced. Cartilage scaffolds have to favour cell adhesion, to promote cellular colonization throughout the structure preserving its stiffness to mimic native cartilage tissue. Materials chosen in this work are hydrogels,

they form a three-dimensional network made of hydrophilic polymers able to absorb water [55]. Poly(ethylene oxide)-dimethacrylate and poly(ethylene glycol) semi-interpenetrating network, has been proved a good cartilage substitute for its high water content, its biocompatibility and stifness [56]. Mesenchymal stem cells seeded onto hydrogel obtained from hyaluronic acid and TGF-β3, produced more proteoglycans and collagen type II than collagen type I an X [57]. A good scaffold has to be stable till extracellular matrix formation and then it has to degrade without leaving toxic substances. A bone scaffold, has to show mechanical properties suited to the implant site; in vitro its stiffness has to be able to load required weight and it should present a certain porosity degree to let cells growth, while in vivo the stiffness scaffold, because bone suffers a physiological stress (compression, torsion and flexion), has to keep tissue intact till its full regeneration [58]. Surface properties of the scaffold affect its bioactivity and osteoconductivity. Osteoconductivity is a process that allows osteogenic cells to migrate onto scaffolds thanks to fibrin clot formed after scaffold implant. During cell migraton there is a fibrin retraction that may cause detachment. So it's important fibrin anchorage and it is favored on rough surface rather than on a smooth one.

3.1.1 Young's modulus

For a mechanical characterization, a force or a moment is applied to a sample, with a precise shape, usually a cylinder or a strip. Force, applied as a compression or a traction, produces a deformation ΔL without changing sample shape. A material is called elastic, when a small force is applied and it deforms reversibly, in other words the material recovers its shape after the force is removed. Usually there is a limit value of stress, over which deformation becomes irreversible and material behaviour is called plastic. Young's modulus is a measure of the stiffness of an elastic material. It is defined as the ratio of the uniaxial stress over the uniaxial strain in the range of stress in which Hooke's Law holds. The slope of the stress-strain curve at any point is called the tangent modulus. The tangent modulus of the initial, linear portion of a stress-strain curve is called Young's modulus. It can be experimentally determined from the slope of a stress-strain curve created during tensile tests performed on a sample. In anisotropic materials,

bone is one of them, Young's modulus may have different values depending on the direction of the applied force with respect to the material's structure. Young' s modulus is also called elastic modulus, and it it the most common elastic modulus used, but exists other moduli like bulk modulus and shear modulus. Young's modulus is the ratio of stress, which has units of pressure, to strain, which is dimensionless; therefore, Young's modulus has units of pressure.

3.1.2 Stress-strain curve

The stress–strain curve is a graphical representation of the relationship between stress, derived from measuring the load applied on the sample, and strain, derived from measuring the deformation of the sample, i.e. elongation, compression, or distortion. The slope of stress-strain curve at any point is called the tangent modulus; the slope of the elastic (linear) portion of the curve is the Young's modulus. The nature of the curve varies from material to material. The following diagram (fig. 3.1.1) illustrates the stress–strain behaviour of typical materials in terms of the engineering stress and engineering strain where the stress and strain are calculated based on the original dimensions of the sample and not the instantaneous values.

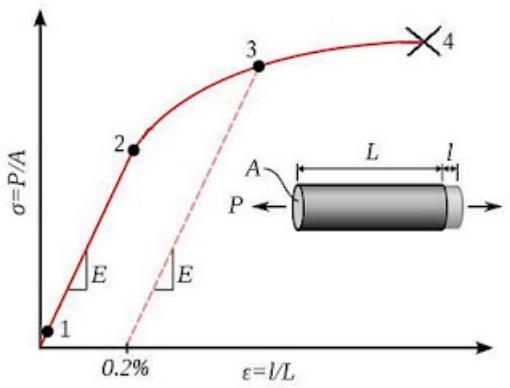

Figure 3.1.1: *Stress-strain curve: stress σ as function of strain ϵ. 1) true elastic limit; 2) proportionality limit; 3) elastic limit; 4) offset yield strength.*

3.2 Experimental section

3.2.1 Scaffold preparation

Cartilage scaffolds with 2.5% w/w GP

A series of hydrogel constructs with different crosslinking agents and realised with several methods were compared, to asses the best scaffold. Hydrogels used were 5% w/v gelatin type A solution, 2mg/ml collagen type I acid acetic solution, and 1% w/v agarose aqueous solution previously described. Crosslinking agents used were besides genipin, EDC/NHS plus DMEM (Dulbecco's Modified Eagle's Medium) culture medium.

Collagen matrix constructs

A set of collagen samples were crosslinked with DMEM culture medium and 0.002 M EDC: 0.05 M NHS solution, and another set with genipin. In the first method, DMEM was added to the collagen solution in a 1:9 weight ratio and rested for one hour in order to complete the cross-linking reaction. After that, the supernatant was removed. DMEM induces a weak collagen cross-linking, unstable in physiological solution [59]. In fact, the cross-linking reversibility can be activated increasing the solution pH from 2.9 to basic values. To avoid this problem, the gel obtained after initial DMEM cross-linking was dipped in 0.05M EDC : 0.0002 NHS solution for 4 hours. At the end, EDC:NHS solution was removed and an excess of a 0.1M Na_2HPO_4 (Sigma-Aldrich, Italy) solution in water was added for 1 hour to obtain an uniform gel. The resulting collagen gel was rinsed for 30 minutes in milliQ water to remove all impurities. This method was adopted to realize cross-linked collagen (CC) constructs. In the second method, 2.5% (w/w) Genipin, calculated respect to the weight of collagen solution, was added. The mixture was heated at 40°C under continuous stirring until the cross-linking process started. This solution was cast on a Petri dish and rested at room temperature for 48 hours. This method was used to cross-link both gelatin and collagen.

Agar matrix constructs

Agar solution in water was used pure or mixed with collagen (crosslinked and not) in 1:1 weight ratio. The three solutions were casted in 29 mm diameter Petri dishes, so three samples were realized: pure agar (A), agar and not cross-linked collagen (ANCC) and agar and cross-linked collagen (ACC) with DMEM and EDC-NHS. Because agar starts to gel at 45 °C, the collagen was added to it at around 36 °C, thus avoiding the collagen denaturation. Samples were hermetically closed to prevent dehydration and stored in fridge at 4 °C.

Gelatin matrix constructs

5% gelatin solution was cross-linked by adding 2.5% (w/ w) GP, respect to the gelatin solution weight. Three series of samples were realized by casting Gelatin and GP solution (G), Gelatin and GP solution mixed with not cross-linked collagen (GNCC), and Gelatin and GP solution mixed with pre cross-linked collagen (GPCC). The GNCC solution was obtained by mixing collagen and gelatin solutions in a 1:1 weight ratio (1g of collagen solution was added to 1g of gelatin solution) at about 36 °C and adding 2.5% GP, respect to total weight of solution. GPCC solution was obtained by mixing 1g of gelatin solution to 1g of DMEM EDC-NHS pre cross-linked collagen and then 2.5% (w/w) GP was added respect to whole weight of the mixed solution. After 48 hours of casting all samples were uniform and mechanically stable.

Cartilage scaffolds with lower GP concentration

Cartilage scaffolds based on 5% gelatin and 2mg/ml collagen were prepared with lower GP concentration. Samples were prepared mixing 5% gelatin and 2 mg/ml collagen solutions in a 1:1 weight ratio (i.e 1g of gelatin with 1g of collagen) in a water bath at 40°C, then GP ad different concentration 0.1%, 0.2%, 0.5% w/w respect to the to total weight of solution was added. The mixture was stirred till the reaction started, blue appeared. On these scaffolds were performed genipin release test as previous described and gelatin release, while Young's modulus was obtained from compression tests conducted using Zwick/Roell mod. Z005 (Zwick GmbH & Co, Germany).

Bone scaffolds with 2.5% GP content

Agar + hydroxyapatite (AHA) constructs were made by adding 43,7% w/v of hydroxyapatite (HA) to the 1% w/v agar solution (A), before the beginning of the gelification process of the latter. Agar + not cross-linked collagen + hydroxyapatite (ANCCHA) constructs were obtained by mixing 1% w/v agar solution with not cross-linked collagen solution in 1:1 weight ratio (ANCC) and then adding 43,7% w/v of HA. Gelatin + GP + hydroxyapatite (GHA) constructs were obtained by adding 43,7% w/v of HA to the 5% w/v gelatin solution , then GP was added on the base of the weight of gelatin solution (2.5 % of the weight of G) to allow the cross-linking process on continuous stirring. Gelatin + not cross-linked collagen + hydroxyapatite (GNCCHA) constructs were obtained by mixing the collagen solution with the 5% w/v gelatin solution in 1:1 weight ratio (GNNCC) on a stirrer in a water bath at about 36 °C and then adding 43,7% w/v of hydroxyapatite. Then GP was added on the base of the weight of GNCC solution (2.5 % of the weight of GNCC) to allow the cross-linking process. All samples are then casted in 29 mm diameter Petri dish for 48 hours.

Bone scaffolds with lower GP concentration and higher HA content

Different samples were prepared, varying hydroxyapatite concentration from 30% to 90% w/v, respect to whole volume of liquid components. For each concentration, samples were prepared according to two different protocols that differ only in the sonication process, finalized to better fragment and disperse HA crystals within hydrogel matrix. A Vibra-CellTM (Sonics & Materials, CT, USA) ultrasonic probe was used for this purpose. In both cases, the components of the samples are the following:

- 10% w/v gelatin solution in milliQ water;
- PBS (Phosphate Buffered Saline) solution, added in a 1:1 volume ratio, respect to the gelatin solution volume;
- 2 mg/ml of collagen solution, added in a 2:1 volume ratio, respect to the gelatin solution volume;

- HA, properly added in order to obtain composites with HA concentrations ranging from 30 to 90% w/v, respect to whole volume of liquid components;
- GP, added in a 0.5% w/v ratio, respect to the whole volume of liquid components.

The first series of samples (protocol 1) were prepared mixing HA powder within the PBS solution at room temperature, then sonicating this mixture at 0.2W for 2 minutes. 2mg/ml collagen acid acetic solution was added to the gelatin solution in a 2:1 volume ratio, and finally the previous prepared HA/PBS mixture was added in a 1:1 volume ratio respect to gelatin solution volume. At the end, GP was added to all mixture in a 0.5% w/v ratio, respect to the whole volume of its liquid components. The final mixture was stirred at 40 °C until the beginning of cross-linking process. The other protocol (protocol 2) provides the sonication of whole mixture, rather than just HA/PBS ones. So all components were mixed according to previous ratios and the final mixture was sonicated for 2 minutes at 0.2 W. In both protocols, samples were left at room temperature either for 48 hours or 10 days.

3.2.2 Collagen release

Collagen released by samples into surrounding aqueous environment was analyzed with UV spectrophotometry (OMEGAstar - BMG Labtech, Italy). A 2.9 cm diameter and 4.5 mm height cylindrical sample was completely dipped in a Petri dish containing 60 ml of deionized water. At different times (1m, 2m, 5m, 10m, 15m, 30m, 1h, 2h, 4h, 8h, 24h) 0.5 ml of water bath was sampled and analyzed at 225 nm with an UV-Vis spectrophotometer.

3.2.3 Genipin Release

Genipin release was performed only for GNNC. Samples with 6 mm diameter and 13 mm height, were put in a test tube containing 10 ml of PBS, mantained at 37°C for 8 days and every day genipin content was analysed with UV spectrophotometry at 244 nm.

3.2.4 Swelling tensile stress-strain and creep tests

Tests were performed with the Ugo Basile 7006 isotonic transducer (Ugo Basile, Italy) connected to the MP35 acquisition platform (BIOPAC Systems Inc, Italy). The Swelling test allows the evaluation of swelling of a sample dipped in water. Once the initial length l_0^{real} was measured, the sample was placed in a Petri dish and mounted on the transducer, so its deformations were measured. The sampling rate was fixed at 1 Hz. After one minute of acquisition with no load, the offset was evaluated and the Petri plate was filled with deionized water until the sample was completely covered. So, the measured time-dependent deformation was equal to:

$$\varepsilon(t) = \frac{l^{real}(t) - l_0^{real}}{l_0^{real}} \tag{3.2.1}$$

where $l^{real}(t)$ is obtained by adding the offset to the measured length $l(t)$ so it represents the elongation of the sample at time t. The test was performed until a stable plateau was reached, so the swelling time constants were derived for each sample through the analysis of the obtained data. Stress-strain test allows the assessing of Young modulus of each sample. The sampling time was the same of the previous test. The weights were applied every 3 minutes, until a maximum weight of 500g. Elastic moduli were evaluated as stress-strain behavior. Creep test was performed in aqueous barh after the swelling test on each sample, so as to have stabilized its original length. In this way the initial length of the sample was equal to:

$$l_{0,creep}^{real} = l_0^{real}(1 + \varepsilon_{endswelling}) \tag{3.2.2}$$

where l_0^{real}, is the initial length of sample and $\varepsilon_{endswelling}$ was the deformation reached in the plateau area after swelling. The sampling frequency was fixed at 2 Hz. The weight necessary to cause 1% linear deformation of a sample was derived from its stress-strain graph.

3.2.5 Dynamic loading test

Dynamic loading tests were performed with GABO Eplexor®150N (GABO-QUALIMETER Testanlagen GmbH, Germany). The elastic modulus in compression (not the Young modulus obtained from stress-strain tests) can be written

as:

$$E^* = E' + iE''$$

where E' is the elastic component ("storage modulus") and E'' the dissipative one ("loss modulus"). The transition from the elastic behavior to the beginning of viscous phenomena can be determined by:

$$tan\delta = \frac{E''}{E'}.$$

Following parameters were adopted in the setup of experiment:

- Contact force: 0.10 N;
- Static load: one that causes a 2% static strain on the sample;
- Static and dynamic load max forces: 1.50 N;
- Static and dynamic load tolerance: 0.50%;
- Temperature: 25°C;
- Temperature tolerance: 2.00°C;
- Sweep type: log;
- Frequency sweep: 0.1 to 100 Hz (20.67 Hz/dec);
- Number of sampling: 63.

Each sample presents a cylindrical shape with 11 mm diameter and 5 mm height.

3.2.6 Compression stress-strain

Tests were performed using Zwick/Roell mod. Z005 (Zwick GmbH & Co, Germany) controlled in position. Realized samples (6 mm diameter with a thickness of 13 mm) maintained in PBS were subjected to a compressive load with the following settings:

- strain rate: 0.07 mm/s;

- end of loading phase: 10% strain (respect of the initial sample length).

Then elastic moduli were calculated from the first linear tract of stress-strain curve.

3.2.7 Genipin release

Realized scaffolds 6 x 6 mm square with a thickness of 2 mm were dipped in 10 ml of PBS and incubated at 37°C to evaluate release of unreacted genipin. 200 µl of soaking solution were daily collected for 7 days and analyzed using an ultraviolet-visible light spectrophotometer (OMEGAstar - BMG Labtech, Italy) at 244 nm.

3.2.8 Load unload cyclic tests

Load-unload tests were conducted using Zwick/Roell mod. Z005 (Zwick GmbH & Co, Germany) controlled in position. Realized samples (6 x 6 mm with a thickness of 5 mm) were subjected to two consecutive compressive load-unload cycles at T=25 °C with the following settings:

- strain rate: 0.07 mm/s;
- end of loading phase: 15% strain (respect of the initial sample length);
- end of load-unload cycle: no load.

3.2.9 SEM and SEM-EDX

SEM (Scanning electron microscopy) and SEM-EDX (Scanning electron microscopy-energy dispersive xray micro-analysis) were performed only on dried samples were mounted on aluminium stubs and then covered with Au by the Edwards Sputter Coater B150S equipment. They were observed with a Philips XL20 microscope (Royal Philips Electronic, Eindhoven, The Netherlands). SEM-EDX is an analytical technique used for the elemental analysis or chemical characterization of a sample.

3.3 Results

3.3.1 Collagen release

Cartilage scaffolds and bone scaffolds

Spectrophotometric analysis showed that no collagen was released from the scaffold matrix into the surrounding aqueous environment. According to this evidence, no graphs are showed in this paper.

3.3.2 Genipin release

Cartilage scaffolds

Considering that genipin toxic concentration tested on osteoblast cultures was established to be 80 µg/ml [60], biocompatibility could be assessed only for scaffolds crosslinked with 0.2% and 0.1% w/w GP concentrations figure 3.3.1.

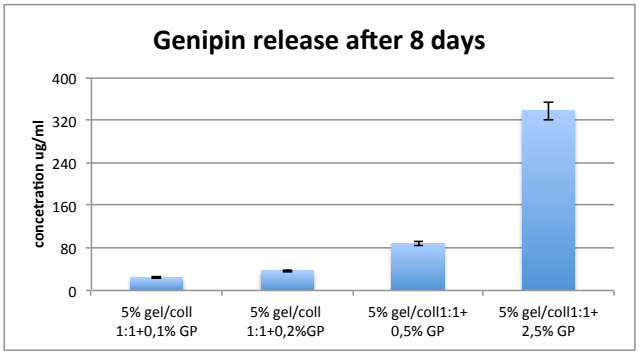

Figure 3.3.1: *Genipin release from cartilage subsitutes after 8 days.*

Bone scaffolds

Results showed that GP released from all samples ranging from 60% to 90% w/v HA concentrations and crosslinked with 0.5% w/w GP, prepared with two different protocols, were under GP toxic value figure 3.3.2 on the next page. Respect to cartilage scaffolds, bone scaffolds with 0.5% w/w genipin concentration

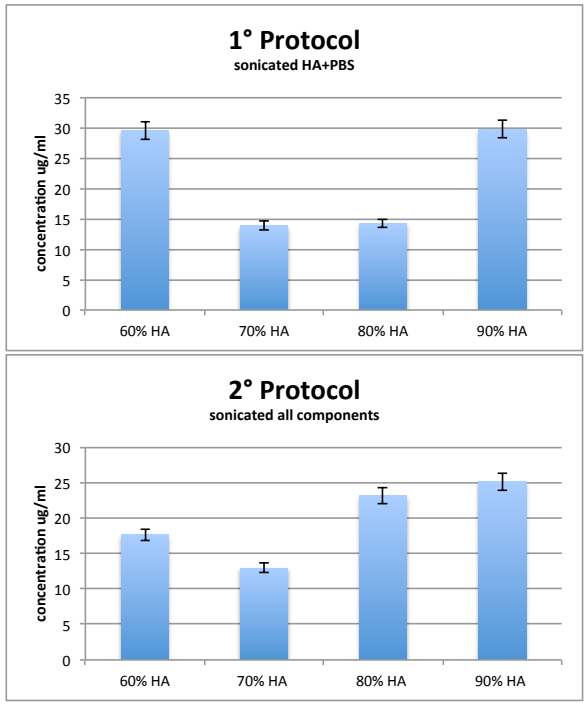

Figure 3.3.2: *GP release from bone scaffolds (0.5% w/w GP) after one week, prepared with two different protocols.*

were not toxic thanks to sonication introduced in their preparation, that favour GP reaction crosslinking, so reducing GP unreacted.

3.3.3 Stress-strain test

Cartilage scaffolds

From stress-strain graphs (fig. 3.3.3 on the facing page) it is possible to note that all samples with 2.5% w/w GP content present an elastic behavior. Elastic moduli of constructs obtained by adding cross-linked or not cross-linked collagen inside gelatin or agar matrix are lower than those of pure matrices (figure 3.3.4 on the next page). It could be due to the overall steric dimensions of collagen constructs and not crosslinked collagen included in the polymeric matrix.

(a)

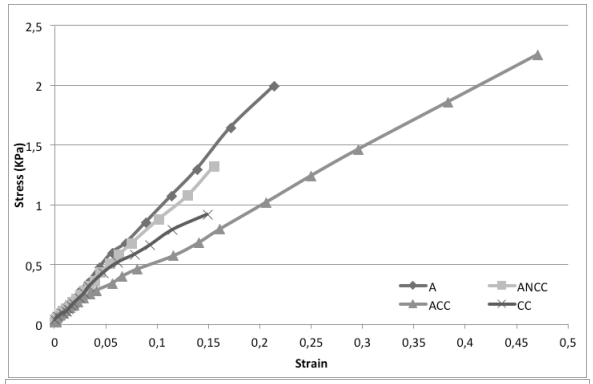

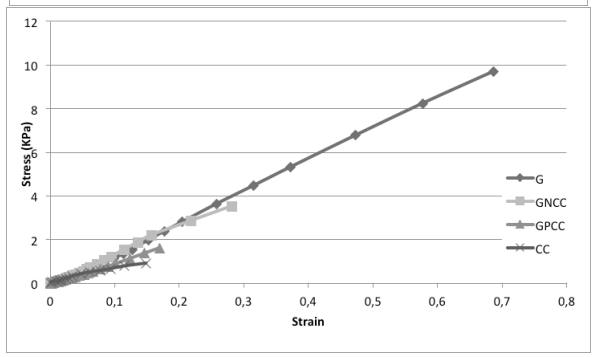

(b)

Figure 3.3.3: *(a) Stress-strain curves of agar matrix samples; (b) Stress-strain curves of gelatin matrix samples.*

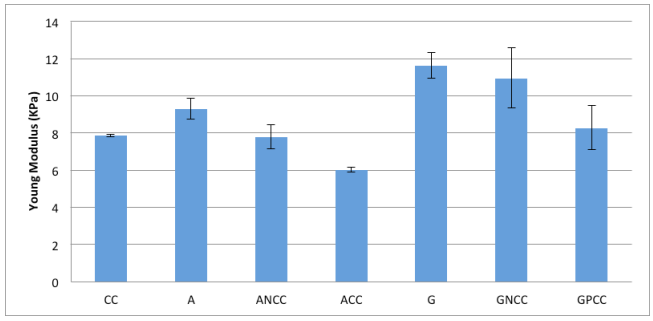

Figure 3.3.4: *Young's moduli of agar and gelatin samples with 2.5% GP content.*

Young's moduli of gelatin samples with 0.2% and 0.5% w/w GP content were almost equal to 2.5% w/w GP samples one, while 0.1% GP samples had a lower modulus value as shown in graph 3.3.5. An explanation could be that already with 0.2% GP content all amino groups were cross-linked, as confirmed by fluorescamine assay in the previous chapter, so increasing GP concentration Young's modulus doesn't change but GP could be only toxic for cells.

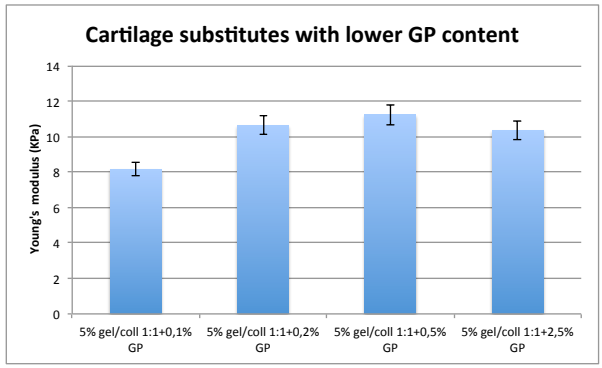

Figure 3.3.5: *Young's moduli of gelatin/collagen samples with lower GP content.*

Bone scaffolds

The presence of collagen in agar and in gelatin+collagen+2.5% GP in bone samples with 43.7% HA, results in an increase in the elastic modulus, table 3.1, as the main effect of collagen in the samples is not to disrupt the network of its matrix, but to interact constructively with crystals of hydroxyapatite (fig. 3.3.6 on the next page).

Bone scaffolds with lower GP concentration and higher HA content
Samples with increasing HA content and lower GP content, realized according both protocol 1 and 2, were mechanically tested 48h and 10 days after their preparation. Furthermore, anisotropy was assessed in samples with 30% and 50% w/v HA, applying a load on both their top and lateral surfaces.

(a)

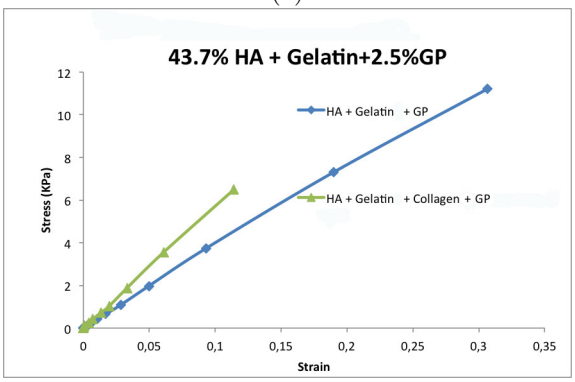

(b)

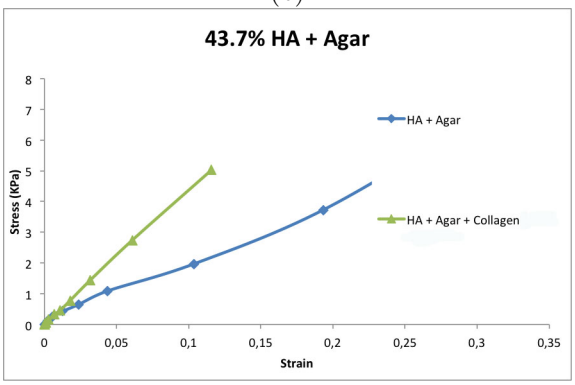

Figure 3.3.6: *(a) Stress-strain curve for bone sustitutes based on gelatin matrix and (b) on agar matrix.*

48h after preparation Elastic moduli of 60%-90% samples realized according to protocol 1 and 2, are shown in fig 3.3.7 on the following page. Samples prepared using ultrasound to mix only HA and PBS, first protocol, showed a strange behavior with increasing HA percentage. 60% HA Young's modulus was greater than the others, even if going from 70% HA to 90% HA samples, modulus had a linear trend. While samples obtained from second protocol, ultrasound applied to the whole mixture, showed an almost linear increasing of Young's modulus with increasing HA content. Data from these graphs suggested that second protocol gave a better HA miscibility reflected in a homogeneous trend of Young's

sample	Young's modulus (kPa)
43.7%HA+agar	25.95
43.7%HA+agar+collagen	44.80
43.7%HA+gel+2.5%GP	39.35
43.7%HA+gel+coll+2.5%GP	57.45

Table 3.1: *Young's modulus of bone substitute based on agar and on gelatin matrix.*

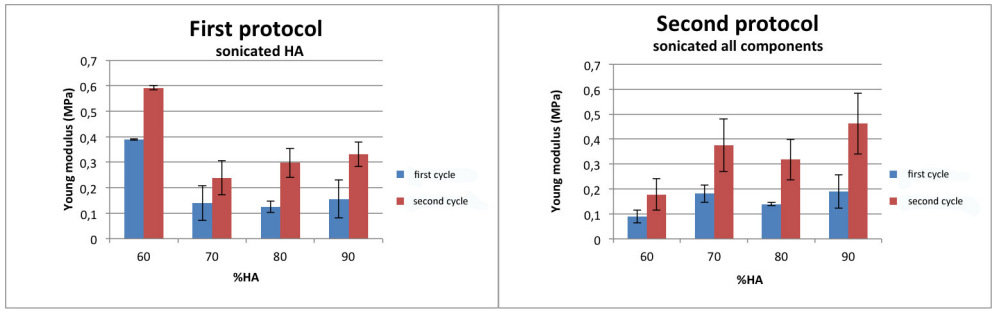

Figure 3.3.7: *Young's moduli for samples after 48h casting, prepared with two different protocols.*

modulus and it results bigger than one of protocol 1 for each HA concentration. Compressive elastic modulus is always greater in the second load-unload cycle especially due to collapse of internal pores and expulsion of residual. On the basis of previous results, lower HA concentrations, 30%, 40% and 50% samples were prepared only with the second protocol. The same trend of higher concentrations was observed (fig. 3.3.8 on the next page). Mechanical anisotropy was assessed in samples with 30% and 50% w/v HA realized according protocol 2. Results are shown in figure 3.3.9 on the facing page.

Similarly to previous results, the elastic modulus increases with the content of HA and it is always greater in the second cycle. Only the sample with 50% (w/v) HA showed a marked anisotropy, resulting more rigid in the tangential direction. This can suggest that there is a threshold HA concentration, above which the polymeric system shows anisotropy. In figure 3.3.10 on the next page,

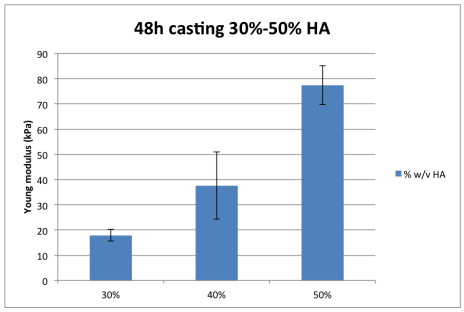

Figure 3.3.8: *Young's moduli for samples after 48h casting, prepared with the second protocol.*

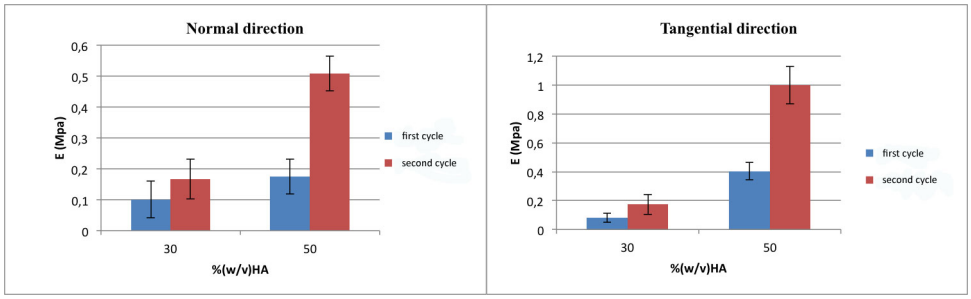

Figure 3.3.9: *Young's modulus for samples after 48h casting calculated in the normal and tangential direction.*

is summarized elastic modulus value for all HA concentrations tested.

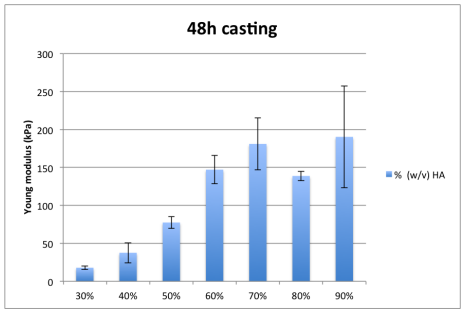

Figure 3.3.10: *Young's moduli for all HA concentrations tested after 48h casting*

10 days after preparation Elastic moduli for samples realized according protocol 1 and 2, are shown in figure 3.3.11. Observations made to discuss pre-

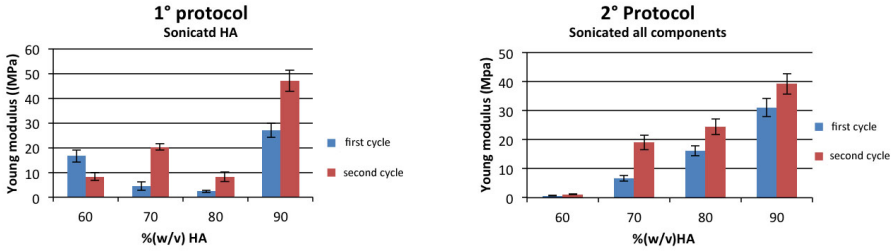

Figure 3.3.11: *Young's moduli for samples after 10 days casting, prepared with two different protocols.*

vious results are again applicable. Note that increased time of casting involves a general tightening of structures, as expected. Studying mechanical anisotropy in 30% and 50% w/v HA samples (realized according protocol 2) ten days after their preparation yielded the following results fig. 3.3.12. The increase of the elastic modulus with HA content and with the second load-unload cycle are confirmed. Again, only the sample with 50% (w/v) HA showed a marked anisotropy, resulting more rigid in the tangential direction. Samples with lower HA content

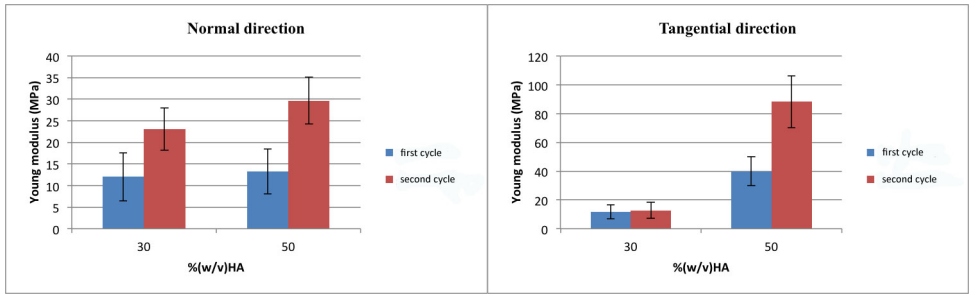

Figure 3.3.12: *Young's modulus for samples after 10 days casting calculated in the normal and tangential direction.*

were prepared only with the second protocol. They showed (figure 3.3.13 on the facing page), as previous samples, a homogenous elastic modulus trend.

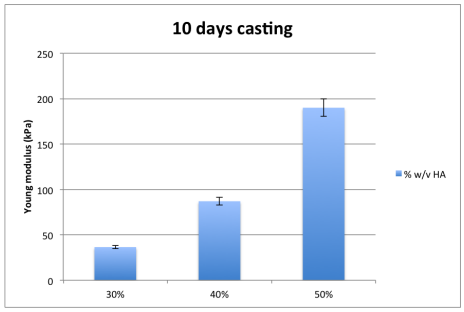

Figure 3.3.13: *Young's moduli for samples after 10 days casting, prepared with the second protocol.*

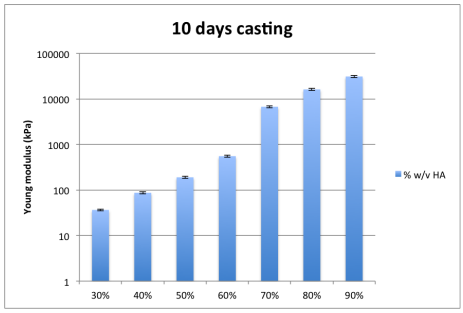

Figure 3.3.14: *Young's moduli of all HA concentration after 10 days of casting. Values on Y axis are in logarithmic form.*

3.3.4 Swelling test

Cartilage scaffolds

From the swelling test analysis, table 3.2, it is possible to note that samples that have gelatin as a matrix did not present swelling. This was due to a complete cross-linking of gelatin that created a structure that was not permeable to aqueous solutions. Instead, samples with agar matrix presented a low swelling relaxation. The swelling was due to the porous structure of the agar matrix and to the presence of CC and NCC which increased the dimension of these pores, and allowed water perfusion within the structure. This hypothesis was confirmed by

sample	final swelling strain (%)	relaxation time (s)
CC	4	2000
A	2.4	8000
ANCC	1.5	1500
ACC	3	1000
G	0	∞
GNCC	0	∞
GPCC	0	∞

Table 3.2: *Swelling results for CC(crosslinked collagen), A(agar), ANCC(Agar+not crosslinked collagen), ACC(agar+crosslinked collagen), G(gelatin+GP), GNCC(gelatin+not crosslinked collagen+GP), GPCC(gelatin+pre crosslinked collagen+GP).*

reduced relaxation times in samples which embed CC.

Bone scaffolds

We did not observed appreciable swelling in aqueous environment for any sample. As example, figure 3.3.15 shows the swelling behavior of 60% HA protocol 1, and it is possible to note only noise centered around zero.

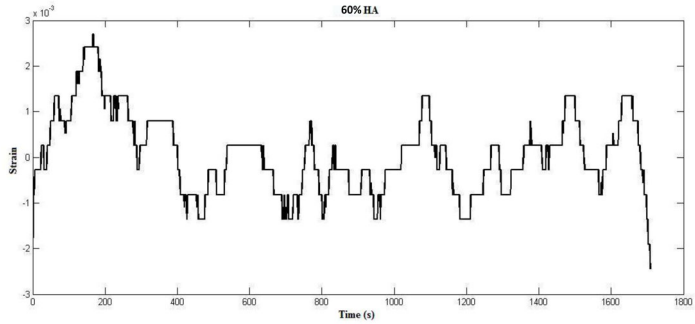

Figure 3.3.15: *Gelatin+collagen+0.5%GP+60% HA sample swelling.*

	CC	A	ANCC	ACC	G	GNCC	GPCC
k_1(kPa)	5.05	32.26	9.68	7.23	101.22	86.16	90.09
k_2(kPa)	2.71	14.13	6.42	5.39	157.50	75.50	54.22
η (kPa·s)	83.95	158.39	74.21	144.07	2148.30	17667.00	13934.54
τ (s)	30.98	11.21	11.56	26.73	13.64	234.00	257.00

Table 3.3: *Calculated coefficients for cartilage creep test.*

3.3.5 Creep test

Cartilage scaffolds

The tested materials showed a mechanical behavior describable with the Kelvin model, expressible as:

$$\varepsilon = \varepsilon_{spring} + \varepsilon_{Voigt} = \frac{\sigma_0}{k_1} + \frac{\sigma_0}{k_2}\left(1 - e^{\frac{-t}{\tau}}\right). \tag{3.3.1}$$

This model fits very well with the obtained experimental data (fig. 3.3.16 on the following page). From table 3.3, it is possible to note that the elastic constants (k_1, k_2) are similar to the experimental elastic moduli. It is possible to note that the elastic constants (k_1, k_2) are similar to the experimental elastic moduli. In addition, samples with agar matrix show a short creep time due to the large water content within them. The presence of cross-linked and not cross-linked collagen produces a considerable increase in viscosity η. This fact could be explained by the theory of "recruitment of the fibers" [61]. Collagen fibers are arranged in a complex structure, thus their alignment along the direction of traction is a slow and gradual process which results in an increase in viscous behavior. This aspect explains why samples with gelatin matrix have the highest constant of viscosity (and longest characteristic creep time) when collagen was embedded in them respect to pure cross-linked gelatin.

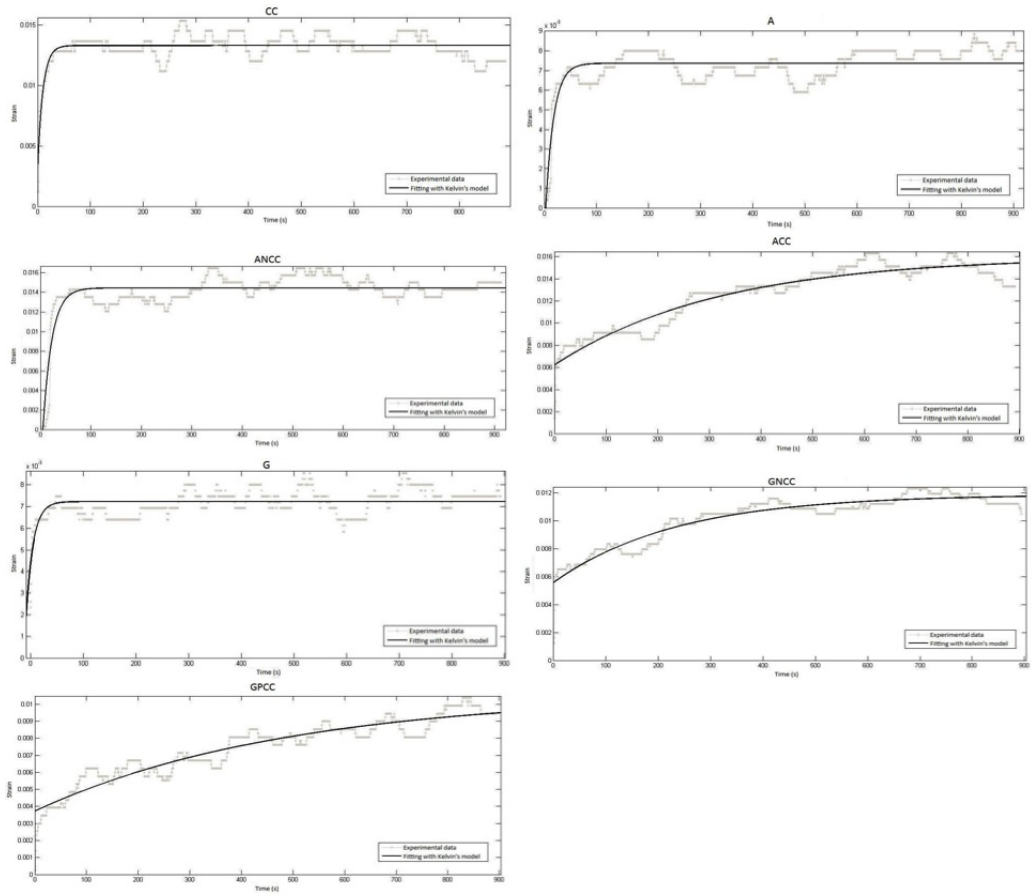

Figure 3.3.16: *Creep experimental data with fitting curve for CC(crosslinked collagen), A(agar), ANCC(Agar+not crosslinked collagen), ACC(agar+crosslinked collagen), G(gelatin+GP), GNCC(gelatin+not-crosslinked collagen+GP), GPCC(gelatin+pre-crosslinked collagen+GP).*

Bone scaffolds

Also these materials showed a mechanical behavior similar to the Kelvin model equation 3.3.1, this model fitted very well the experimental data obtained fig. 3.3.17 on the next page. The obtained results are summarized in table 3.4 . If compared with stress-strain data, it is possible to note similarities between the elastic con-

stants values (k_1 and k_2) and the experimental elastic moduli (Young's moduli). The presence of hydroxyapatite led to a much more compact structure characterized by a predominantly elastic behavior, so the results show low viscosity constants and, consequently, a relatively short characteristic creep time.

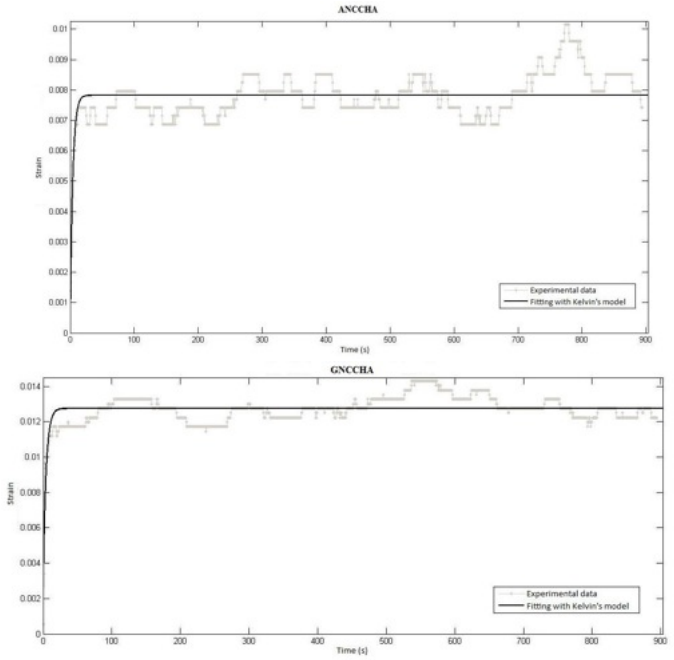

Figure 3.3.17: *Creep test with fitting curve for ANCCHA (agar+not-crosslinked collagen+43.7%HA) and GNCCHA (gelatin+not-crosslinked collagen+2.5%GP+43.7%HA).*

3.3.6 Dynamic loading test

Cartilage scaffolds

All samples demonstrated a marked increase in the compression modulus with increasing deformation rate. At high-speed deformation samples have an elastic behavior, while for low-speed deformation their behavior is similar to a viscous liquid. This trend in compression modulus is justified because polymeric chains

	ANCCHA	GNCCHA
k_1(kPa)	482.50	163.95
k_2(kPa)	73.82	41.58
η (kPa·s)	349.91	349.91
τ (s)	4.74	4.37

Table 3.4: *Calculated coefficients for bone subsittutes creep test.*

could not orient along the loading direction because of the increase in the frequency of stimulation. Viscous behavior involves inner flows of polymeric chains which is associated with the conversion of mechanical energy into heat, so the temperature rises. For all samples there is a nearly perfect overlap between the "storage" and the overall modulus. For this reason the samples principally present an elastic behavior and, therefore, losses due to viscosity are very limited. The "loss" modulus is significantly lower than the "storage" one in the considered frequency range, and, consequently, tan(δ), the ratio between the "loss" and "storage" modulus, is close to zero. Tan (δ), "loss" and "storage" modulus, are shown for cross-linked collagen and for agar-matrix samples in the 0-10 Hz frequency range fig 3.3.18 on the facing page. Tan (δ) is stable at about 0.1 already at a frequency of 1 Hz, that is the typical frequency value corresponding to normal walking. This result suggests that all samples present an elastic mechanical behavior.

3.3.7 SEM micrographies

Cartilage scaffolds

At 1000x magnification, SEM Micrograph (figure 3.3.19 on page 65) a) shows gelatin fibers cross-linked by genipin. At minor magnification the matrix appears compact. The morphology of GPCC construct is compact and non regular due to protein aggregates (fig3.3.19 b-c). This confirms the mechanical and the swelling results. At high magnification it is possible to note a morphology close to that observed for cross-linked gelatin (fig.3.3.19 d-e).

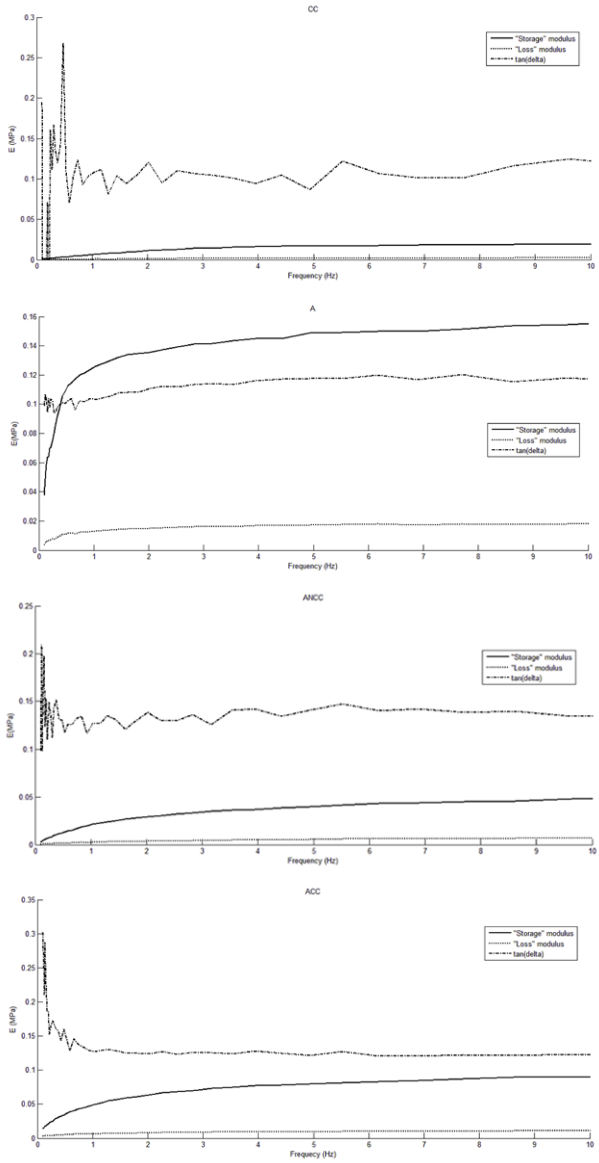

Figure 3.3.18: *Dynamic loading curve of (CC) Cross-linked collagen; (A) Agar; (ANCC) Agar and not cross-linked collagen; (ACC) Agar and cross-linked collagen.*

Bone scaffolds

Surface roughness, observable even at low magnification, is associated with the presence of hydroxyapatite (fig. 3.3.20 a). At higher magnification it is possible to see HA crystals coated and interconnected by gelatin and collagen fibers (fig. 3.3.20 b-c). This evidence confirms the hypothesis that collagen acts as a glue linking together hydroxyapatite crystals.

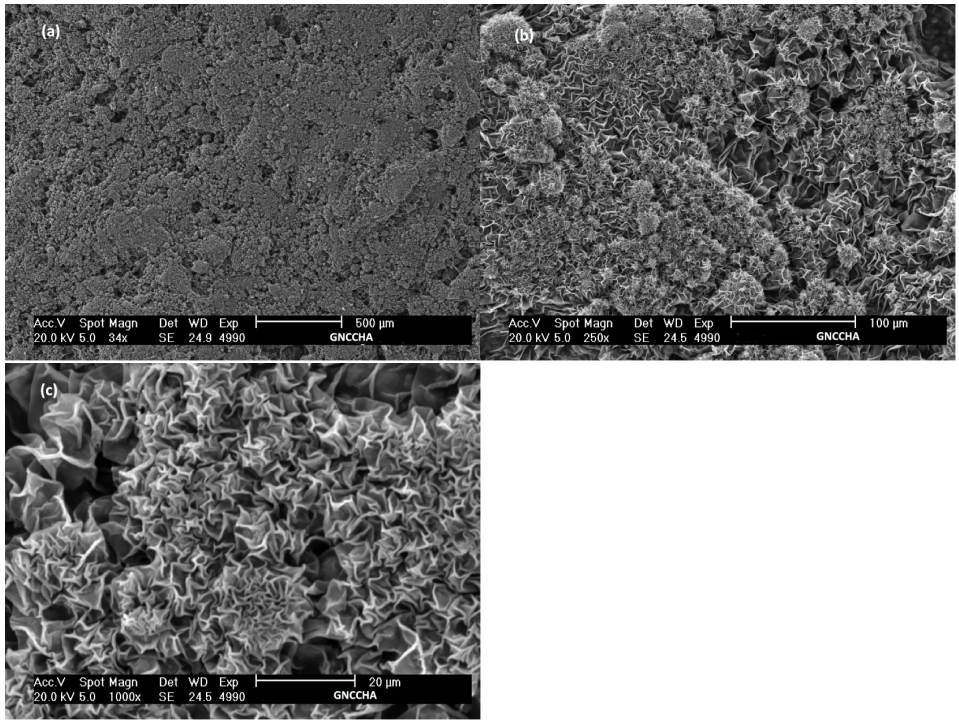

Figure 3.3.20: *SEM micrographs of (a) GNCCHA (gelatin+not-crosslinked collagen+2.5%GP+43.7%HA) at 35x magnification; (b) at 250x magnification and (c) at 1000x magnification.*

3.3.8 SEM-EDX

This non-destructive technique allows the analysis of solid samples that are stable under the operating conditions of low pressure and electron bombardment. EDX

analysis of constructs indicates a uniform distribution of calcium (red in figure 3.3.21) and phosphorus (green in figure 3.3.21). The quantities of the elements, given as weight percentages, are Calcium = 70.28%, Phosphorous = 26.78 % and Magnesium = 2.94%.

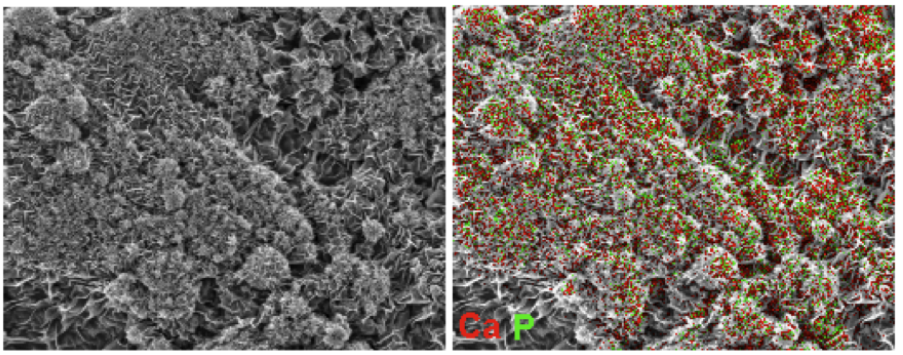

Figure 3.3.21: *SEM-EDX for bone sustitute gelatin+not-crosslinked collagen+2.5%GP+43.7%HA.*

3.4 Conclusions

All scaffolds characterisation can be divided in two experimental parts. In the first part, the genipin concentration used, 2.5% w/w, was decided favouring the rate reaction, but after genipin release assessment this concentration revelead to be toxic for cells. So scaffolds with lower GP concentrations were tested first measuring its release in acqueous enviroment, and then evaluating Young's modulus. As regard cartilage substitutes, reduced GP concentration, till to 0.2% w/w, didn't affect elastic modulus, and scaffolds could re-enter in the biocompatibility range starting from 0.2% GP and going down. While for bone substitutes biocompatibility was already assessed with 0.5% GP concentration, thanks to sonication included in the protocol preparation to improve HA miscibility, especially when HA was present in higher concentrations. Ultrasound were introduced at two different levels giving two different protocols. The best was the protocols including sonication of the entire mixture, that showed a homogeneous trend of elastic modulus. Meanwhile collagen release was absent and also swelling, showing sta-

bility of these structure. All experimental results suggested that 5% w/v Gelatin + not crosslinked collagen 1:1 + 0.2% GP constructs could be used as an innovative hydrogel for cartilage repair. The elastic modulus of the constructs does not mimic that of natural tissue, but their high biocompatibility and the presence of chemo-attractors within them should help to produce fast cell colonization. Adding HA at different concentrations respect to gelatin collagen mixture volume we can modulate elastic modulus on the basis of our needs, considering that Young's modulus of cancellous bone is 0.02-0.5 GPa. From SEM analysis, structures present an uniform distribution of calcium and phosphorous, and HA crystals are interconnected each other by gelatin and collagen. These results suggest that these scaffolds were suitable substitutes for bone regeneration.

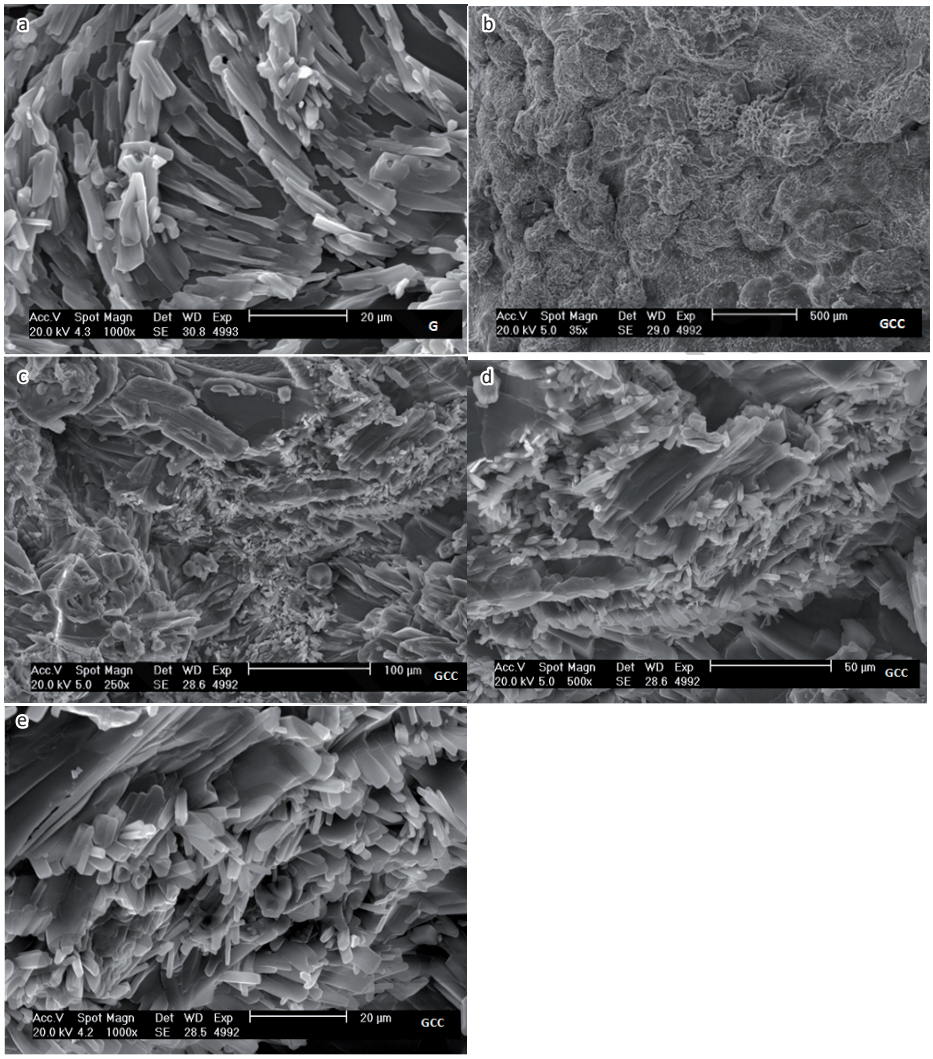

Figure 3.3.19: *SEM micrographs of (a) Gelatin (1000x magnification); (b) Genipin and not cross-linked collagen (35x magnification); (c) Genipin and not cross-linked collagen (250x magnification); (d) Genipin and not cross-linked collagen (500x magnification); (e) Genipin and not cross-linked collagen (1000x magnification).*

4

Discrete graded bone scaffolds

Abstract

In the previous chapter the optimal protocol to prepare bone scaffolds was fixed, here the realization of discrete bone scaffolds and their mechanical characterization will be described. Moreover, scaffold response to different pH will be tested, both for discrete and homogeneous scaffolds.

4.1 Introduction

4.1.1 Gradients in natural structures

The structural organizations found in nature are largely dictated by their functions, load-bearing function, biomechanical function, etc. Simple observations of natural tissues and organs show that these structures are not homogeneous and there exist natural functional gradients in their structure, as seen in the examples of bamboo, mollusc shells and human tissues such as bone and skin [62]. When each layer of the tissue or organ has one or more specific functions to perform and the tissue or organ has more than one layer, the tissue or organ is said to be functionally graded across the layers. Simply, the tissue or organ is described as functionally graded. As such, to regenerate the natural tissue, a successful TE scaffold should also be functionally graded. This is to facilitate the seeded cells

to proliferate at the desired layer and to perform their functions properly and normally to achieve the regeneration of healthy tissues. This can be observed and described from three perspectives: biological, mechanical and anatomical. Matching these perspectives will provide the favourable environment required for cell growth and proliferation for successful organ or tissue regeneration. From a biological point of view, functional gradients are very often observed in human organs and tissues. Different layers of the tissue perform different roles in maintaining the organ functions. One layer may possess cell types or phenotypes that may be different from other layers. A well-engineered TE scaffold should be tailored with the appropriate pore sizes and porosities according to the needs of the specific cells to better accommodate the proliferation and growth of the cells. To drive the neo-tissue to behave like the original tissue, some kinds of mechanical cues are needed [63]. Human bone, observed across its transverse section, has a graded structure varying its pore size and porosity distribution. Its outer layer, cortical bone, is solid and dense, while the inner layer, cancellous bone, is a spongy honeycombed structure filled with blood vessels and bone marrow maximizing the strength to weight ratio for bending and compression loads [62]. As a result, bone structure has functionally graded mechanical properties. Mechanical properties of scaffold should match those of the host tissue, this is particularly important for bone tissues as they are the main load-bearing tissues in the body. For a load-bearing tissue, if the scaffold has superior mechanical properties as compared to those of bone, the scaffold will take the load previously taken by the bone and thus shield the bone from load, causing bone resorption at the surrounding tissue. The opposite scenario of having an inferior scaffold will result in scaffold failure, as the scaffold does not have sufficient strength to withstand the physiological loads [64].

4.1.2 pH during fracture healing

During healing process there is a relevant pH change as shown in figure 4.1.1 on the next page. Cells damage togheter with lactic acid turn pH to acid value. Slowly after 10 days pH rises to physiologic and then reaches basic value when phosphatase activity, responsible for the hydrolysis of esters of phosphoric acid, becomes intense. Maximum basic value is reached after 25 days when mineral

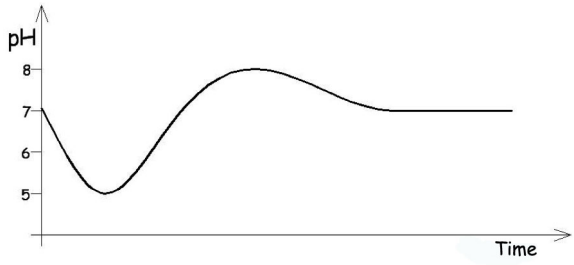

Figure 4.1.1: *pH variation during healing fracture.*

salts starts to precipitate and slowly it returns to neutral pH. These are indicative values and times they depend on subjects. The remodeling process begins at a quiescent bone surface with the appearance of osteoclasts. These are large multinucleated cells that form by fusion of mononuclear precursors of haemotopoetic origin [65]. They attach to the bone tissue matrix and form a ruffled border at the bone/osteoclast interface that is completely surrounded by a "sealing" zone. Thus the osteoclast creates an isolated microenvironment. Subsequently the osteoclast acidifies the microenvironment and dissolves the organic and inorganic matrices of the bone [66]. Briefly after this resorptive process stops, osteoblasts appear at the same surface site.

4.2 Experimental section

4.2.1 Homogeneous and discrete graded samples preparation

Homogeneous scaffolds were prepared according to protocol 2, described in the previous chapter, with 30%, 40%, 50%, 60%, 70%, 80% and 90% HA w/v concentrations followed by 48h or 10 days casting. Discrete graded scaffold were realized stacking mixtures with different HA concentrations, obtained as previously described. Precisely, four different discrete gradient samples were realized, stacking different homogeneous layers characterized by following HA concentrations (both 48h and 10 days casting samples): 30-50%, 60-70%, 80-90% and a

multilayer 30%-40%-50%-60% sample (only after 48h from preparation). The genipin cross-linking process was used to join the different layers. First, the bottom layer with desired HA concentration was prepared, than the second layer (with a lower HA concentration) was cast on it only when genipin cross-linking process started, thus avoiding mixing between layers and allowing, at same time, a parallel cross-linking completion that joins the two different layers.

4.2.2 Buffer solution preparation

Buffer solution pH 5 was an acetate buffer prepared using acid acetid and sodium acetate salt; pH 6 buffer solution was made of hydrogen phthalate/hydrogen phthalate anion, pH 8 was a phosphate buffer made of sodium dihydrogen phosphate/dipotassim phosphate. PBS was pH 7 buffer.

4.2.3 Load-unload cyclic tests

Discrete samples were mechanically tested both 48h and 10 days after their preparation for anisotropy, and homogeneous scaffolds were tested dipped in different buffer solution with pH values 5, 6, 7, 8. Parameters and instrument used were the same of previous chapter: Zwick/Roell mod. Z005 (Zwick GmbH & Co, Germany) controlled in position. Realized samples (6 x 6 mm with a thickness of 5 mm) were subjected to two consecutive compressive load-unload cycles at T=25 °C with the following settings:

- strain rate: 0.07 mm/s;
- end of loading phase: 15% strain (respect of the initial sample length);
- end of load-unload cycle: no load.

4.3 Results

4.3.1 Cyclic compression tests on discrete gradient samples

According to figure 4.3.1 on the facing page, layers react in series when the load is applied in the normal direction (versor n in figure), while they react in parallel

when construct is subjected to a tangential load (versor t in figure). Results for discrete gradient scaffolds are shown as for previous composite homogeneous samples after 48h and 10 days casting.

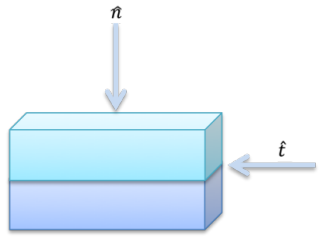

Figure 4.3.1: *Load application to discrete scaffolds.*

48h after preparation Elastic moduli for bi-layered structures are shown in the following figure 4.3.2 on the next page. Only 30%-50% HA discrete gradient sample showed a marked anisotropy, as their two layers react in series or in parallel to the load, depending on its direction of application. Results confirmed that compressive modulus increases as HA total concentration increases and it is always greater in the second cycle for both loading directions. Furthermore, discrete gradient structures were more rigid when their layers are subjected to a tangential load. This evidence was more pronounced within the second cycle, since both layers were stiff due to residual water expulsion and collapse of internal pores. Also multilayer scaffold (figure 4.3.3) showed anisotropy with a bigger elastic modulus for tangential direction after one compression cycle.

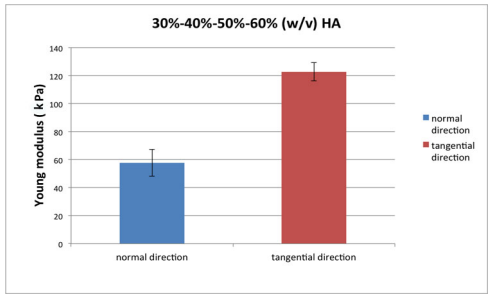

Figure 4.3.3: *Elastic modulus of multilayer scaffold after one compression cycle.*

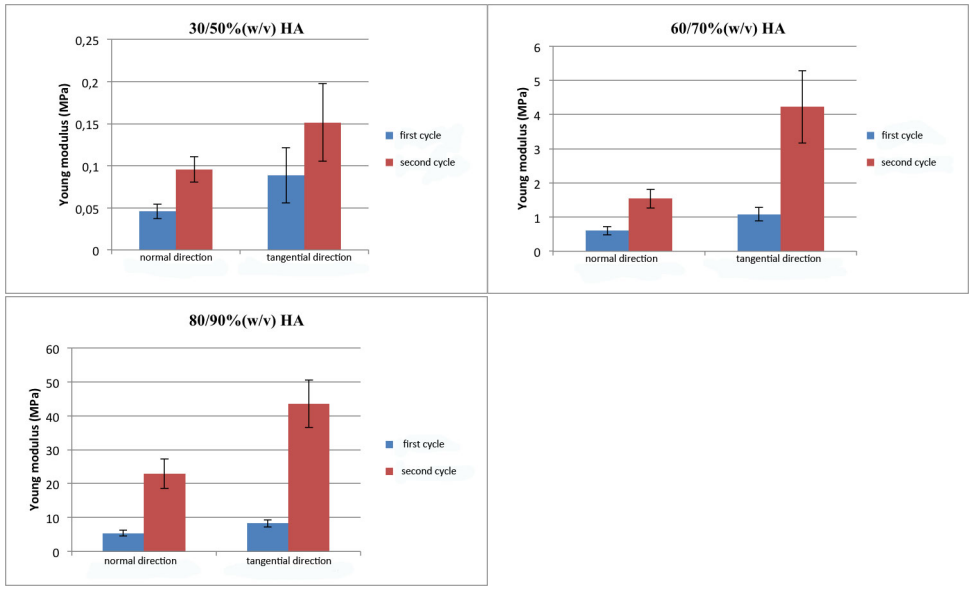

Figure 4.3.2: *Elastic moduli (after 48 hours from preparation) of discrete gradient scaffolds made by homogeneous samples.*

The tested materials showed a mechanical behavior describable with the Kelvin or Reuss models depending on the direction of load application (figure 4.3.4 on the next page). In the Voigt model, the overall Young's modulus $E_{composite}$ of the composite with two constituents 1 and 2 in the specified load direction is given by:

$$E_{composite} = E_1 V_1 + E_2 V_2 \tag{4.3.1}$$

where E is elastic modulus and V is volume fractions of single layer. This model provides an upper bound to the composite stiffness. A lower bound is given by the analogous Reuss model which yields:

$$E_{composite} = \frac{E_1 E_2}{V_1 E_2 + V_2 E_1} \tag{4.3.2}$$

Young modulus obtained from the equations for 30%-50% HA sample, were similar to experimental ones for 48h casting (table 4.1). Elastic modulus eval-

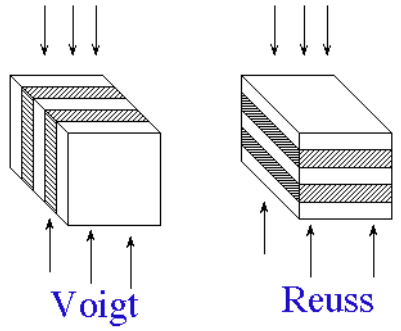

Figure 4.3.4: *Voigt and Reuss models.*

	E_{Reuss}	E_{Voigt}	Exp E_{Reuss}	Exp E_{Voigt}
first cycle (kPa)	36.00	46.8	45.70±8.46	88.60±32.90
second cycle (kPa)	71.3	100.00	95.60±14.90	151.00±46.00

Table 4.1: *Experimental and calculated elastic moduli for 30%-50% HA sample after 48h casting.*

uated for multilayer samples using equations 4.3.1and 4.3.2, and experimental moduli showed in table 4.2 were similar.

E_{Reuss}(kPa)	62.84	Exp E_{Reuss}(kPa)	57.8±9.6
E_{Voigt}(kPa)	132.27	Exp E_{Voigt}(kPa)	123±6.5

Table 4.2: *Experimental and calculated elastic moduli for multilayer HA sample after 48h casting.*

10 days after preparation These samples showed an inverse trend respect to HA increasing content. Elastic moduli decreases with increasing HA and 60%-70% sample didn't show anisotropy (figure 4.3.5). We can suppose that HA undergoes a different rearrangement after water evaporation that leds an irregular elastic modulus trend. For these samples, there no similarity with calculated

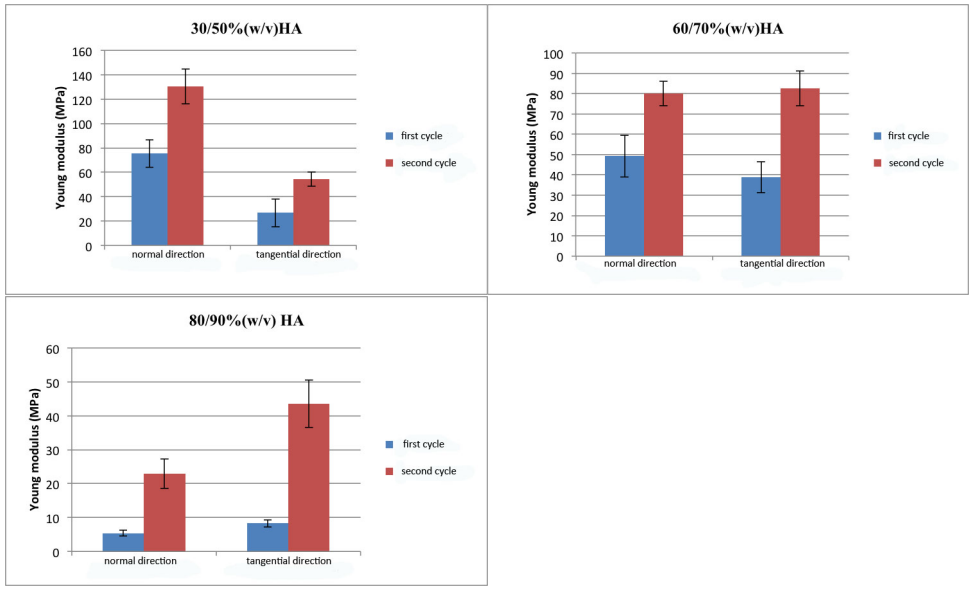

Figure 4.3.5: *Elastic moduli (after 10 days from preparation) of discrete gradient scaffolds made by homogeneous samples.*

and experimental moduli, using Reuss-Voigt equation, due to their strange ex-

perimental behavior (table 4.3).

	E_{Reuss}	E_{Voigt}	Exp E_{Reuss}	Exp E_{Voigt}
first cycle (MPa)	15.8	12.30	75.40±11.30	26.7±11.50
second cycle (MPa)	26.10	29.3	131.00±14.4	54.40±5.94

Table 4.3: *Experimental and calculated elastic moduli for 30%-50% HA sample after 10 days casting.*

4.3.2 Elastic modulus at different pH

48h casting At same pH compressive elastic modulus basically increases as content of HA increases. It increases with increasing pH, it is more evident in high HA samples (fig. 4.3.6). It is because HA, basic material, dissolves at acid pH, so elastic modulus decrease. At same time genipin reaction is favoured at slow basic pH [53], and it gives a higher modulus.

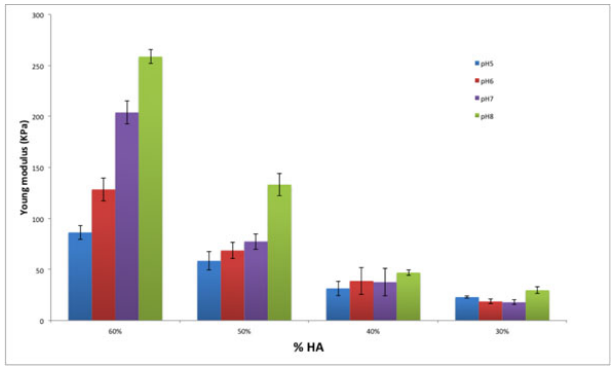

Figure 4.3.6: *Elastic moduli trend at different pH for 48h casting sample.*

10 days casting Homogenoous scaffolds after 10 days had the same trend of 48h casting samples (fig. 4.3.7 on the following page). As aspected Young modulus is greater after water evaporation respect to 48h samples.

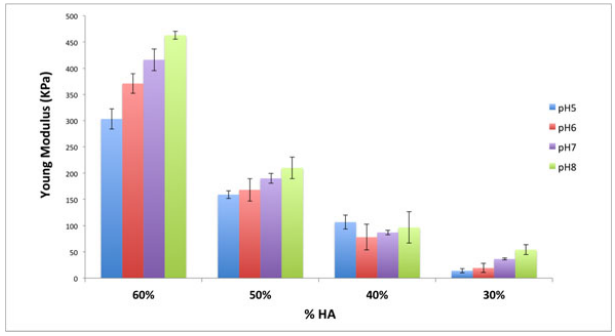

Figure 4.3.7: *Elastic moduli trend at different pH for 10 days casting sample.*

4.4 Conclusions

In this chapter we considered a particular situation that occurs after bone trauma, that is a change in pH value. Elastic moduli of homegenous bone scaffolds ranging from 30% HA to 60% HA were meseaured at different pH (5, 6, 7 and 8) observed during fracture healing. All samples were prepared with the second protocol and tested after 48h and 10 days dipped in different buffer solutions. An increasing pH affected positively Young's moduli both because HA was less soluble in basic conditions, both because genipin could improve long range linking. These behavior was more evident with 60% HA content. Another important bone feature considered in this chapter was its mechanical gradient. A series of discrete gradient scaffolds, three bi-layered and one multilayered, were realized and tested for anisotropy. Only 30%-50% and multilayered HA scaffolds showed anisotropy after 48h of casting, while all 10 days casting samples had an anomalous tendency, reffered to a possible HA rearrangement during water evaporation. Elastic modulus of tangential direction was bigger than assial one, as happens in bone. So these are good candidates for bone substitutes, particular multilayered scaffold.

5

In vitro tests

Abstract

This chapter will deal with preliminary biocompatibility in vitro tests for cartilage and bone substitutes characterized in previous chapters. Primary murine fibroblasts were seeded on cartilage scaffolds and cells viability was analyzed via Alamar assay togheter with DAPI staining, the last only to furnish qualitative data. Bone scaffolds were seeded with MG63 cells (Human osteosarcoma cell line) and cells adhesion and proliferation were observed under SEM.

5.1 Introduction

5.1.1 Genipin biocompability

Genipin, a compound extracted from the fruit, is a traditional medicine for diabetes and raw material for pigment production. Its great potential as a natural crosslinking agent for biomaterials was first reported in 1998: in comparison with glutaraldehyde, genipin exhibited comparable crosslinking capability but significantly lower toxicity. Genipin was first tested to fix biological tissues and glutaraldehyde and an epoxy compound (ethylene glycol diglycidyl ether) were used as controls. It was found that the genipin-fixed tissue had a resistance against enzymatic degradation comparable to the glutaraldehyde-fixed tissue. This sug-

gested that genipin can form stable crosslinked products [67]. In addition, the biocompatibility of the genipin-fixed tissue was studied in a growing rat model subcutaneously [68]. It was noted that the inflammatory reaction of the genipin-fixed tissue was significantly less than its glutaraldehyde- and epoxy-fixed counterparts. The cytotoxicity of genipin was previously studied in vitro using 3T3 fibroblasts, glutaraldehyde was used as a control [35]. The results obtained in the MTT assay implied that genipin was about 10,000 times less cytotoxic than glutaraldehyde. Also, the colony-forming assay suggested that the proliferative capacity of cells after exposure to genipin was approximately 5000 times greater than that after exposure to glutaraldehyde. It was noted that the 3T3 fibroblasts seeded on the surface of the glutaraldehyde-fixed tissue were not able to survive. In contrast, the surface of the genipin-fixed tissue was filled with 3T3 fibroblasts. In addition, neocollagen fibrils made by these fibroblasts were observed on the genipin-fixed tissue. Residues from the genipin-fixed had no toxic effect on the seeded cells while those released form glutaraldehyde-fixed tissue reduced cells population. This indicated that the cellular compatibility of the genipin-fixed tissue was superior to its glutaraldehyde-fixed counterpart. Furthermore a GP-crosslinked gelatin hydrogel is less cytotoxic than a carbodiimide-crosslinked gelatin hydrogel [50]. Cells cultured in the medium containing the fresh sample and in the vicinity of the GP-crosslinked gelatin hydrogel were confluent. In contrast, the cells cultured in the vicinity of the EDC-, EDC/NHS-crosslinked gelatin hydrogels were not as confluent.

5.2 Experimental section

5.2.1 Scaffold sterilization

All scaffolds, cartilage and bone ones, were prepared with protocols explained in chapter 3. Cartilage scaffolds tested were 5% gelatin+2mg/ml collagen 1:1 with 0.2% w/w genipin, while bone scaffolds, besides the same concentrations and ratio of gelatin and collagen, had 0.5% w/w Genipin and different HA concentration that goes from 22,5% to 90% w/v of entire mixture. Collagen and gelatin and all instruments were sterile, preparation was carried out in a laminar flow hood.

About 250 µl of mixture was put in a 24 well plate and then in a humidified incubator at 37°C, using a standard mixture of 95% air and 5% CO_2 for two days to complete crosslinking. After casting scaffolds were washed with EtOH 70%, PBS, and finally exposed to UV for 30' to be sure to sterilize them. The scaffolds were pre-wetted in the culture medium overnight before seeded.

5.2.2 Cell culture and seeding

Cartilage scaffolds A vial of cryopreserved fibroblast primary murine cells was thawed and plated and cultered with Dulbecco's modified Eagle's medium 4.5 g/l glucose (Lonza, Milan, Italy) supplemented with 10% fetal bovine serum (FBS), 1% L-glutamine (Lonza, Milan, Italy), and 1% Penicillin-Streptomycin-Amphotericin B Mixture (Lonza, Milan, Italy). They were grown in a controlled atmosphere (5% CO2; T=37°C) and at confluence they were split 1:6 and used at five passage. Cells were detached using 0.25% trypsin (Lonza, Milan, Italy) and seeded (in triplicate) onto scaffolds and in wells coated with a mixture 1:1 of 5% gelatin+ 2mg/ml collagen as controls at a density of $1 \times 10^{4 cells}/_{cm^2}$. Scaffolds (in triplicate) only with media culture, without cells, were used as blank. They were cultured for 3 days.

Bone scaffolds MG-63 human osteoblast-like cells (ATCC, Rockville, MD) were grown in a controlled atmosphere (5% CO_2; T=37°C) in Dulbecco's modified Eagle's medium 4.5 g/l glucose (DMEM; Sigma, Milan, Italy) supplemented with 10% fetal bovine serum (FBS), 1% L-glutamine (Sigma), and 1% antibiotics (penicillin–streptomycin; Gibco-Invitrogen, Milan, Italy). After thawing, they were routinely split 1:10 every 2–3 days. MG-63 cells were detached using 0.25% trypsin in 1 mM EDTA (Sigma) and seeded (in triplicate) onto scaffolds at a density of $1 \times 10^{4 cells}/_{cm^2}$. They were cultured for 2 days.

5.2.3 Alamar blue assay

After seeding, Alamar blue assay, cell viability assay, (The CellTiter-Blue®„ Promega, Italy) was performed every day to asses cartilage scaffold biocompatibility. Alamar assay provides a homogeneous, fluorometric method for estimat-

ing the number of viable cells. It uses the indicator dye resazurin to measure the metabolic capacity of cells, an indicator of cell viability. Viable cells retain the ability to reduce resazurin into resorufin, which is highly fluorescent ($579_{Ex}/584_{Em}$). Nonviable cells rapidly lose metabolic capacity, do not reduce the indicator dye, and thus do not generate a fluorescent signal. The fluorescence produced is proportional to the number of viable cells. The medium was removed from all samples (including controls and blanks) and replace with fresh one, then Alamar solution was added in an amount equal to 10% of the culture medium volume according to the manufacturer's instructions. Aliquots were transferred to a 96-well plate after 30' and 2h 30', and the fluorescence was recorded using spectrofluorimeter (OMEGAstar - BMG Labtech, Italy). The viability was expressed as percent fluorescence of samples respect to controls.

5.2.4 DAPI staining

At the end of third day, cells were immediately fixed in 10% formaldehyide in PBS for ten minutes and stained with DAPI (4', 6-diamino-2-phenyldione) (Sigma, Milan, Italy) for 5 minutes and observed under a fluorescence microscope. DAPI can pass through an intact cell membrane and binds strongly to A-T rich regions in double stranded DNA. For fluorescence microscopy DAPI is excited with ultraviolet light and is detected through a blue/cyan filter.

5.2.5 SEM and SEM-EDX

SEM and SEM-EDX were performed only for bone scaffolds at the end of two days MG63 culture. Samples were fixed in 2% glutaraldehyde (Sigma) in 0.1M cacodylate buffer (pH 7.4, Sigma), postfixed in 1% osmium tetroxide (Sigma), dehydrated in increasing ethanol (Sigma) concentrations, CPD (critical point drying)-dried, mounted on aluminium stubs, and gold-sputtered with the Edwards Sputter Coater B150S equipment. They were observed with a Philips XL20 microscope (Royal Philips Electronic, Eindhoven, The Netherlands).

5.3 Results

5.3.1 Cell viability

In figure 5.3.1 fibroblast viability after 3 days is showed. Viability of fibroblasts seeded on scaffolds, expressed as percent fluorescence respect to fibroblasts seeded on well coated with gelatin collagen (control), was inferior to 50% during the first day, but then it raised during the second days to reach control value at the end of experiment. During the third day there was a small decrease in control viability due to confluence. Initially cells needed a period to adapt to a new substrate, from this derives a low viability during the first day of experiment. Similar

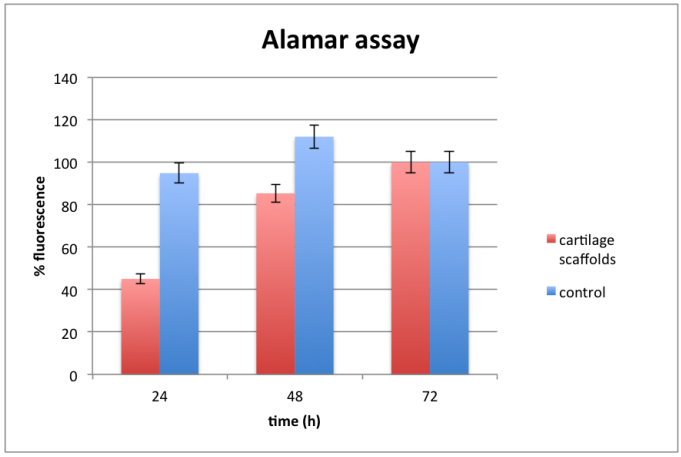

Figure 5.3.1: *Fibroblasts viability seeded on cartilage scaffolds respect to control*

cellular density at the third day was confirmed by DAPI staining (figure 5.3.2 on the following page). There are not so differences between cells on scaffolds and control cells.

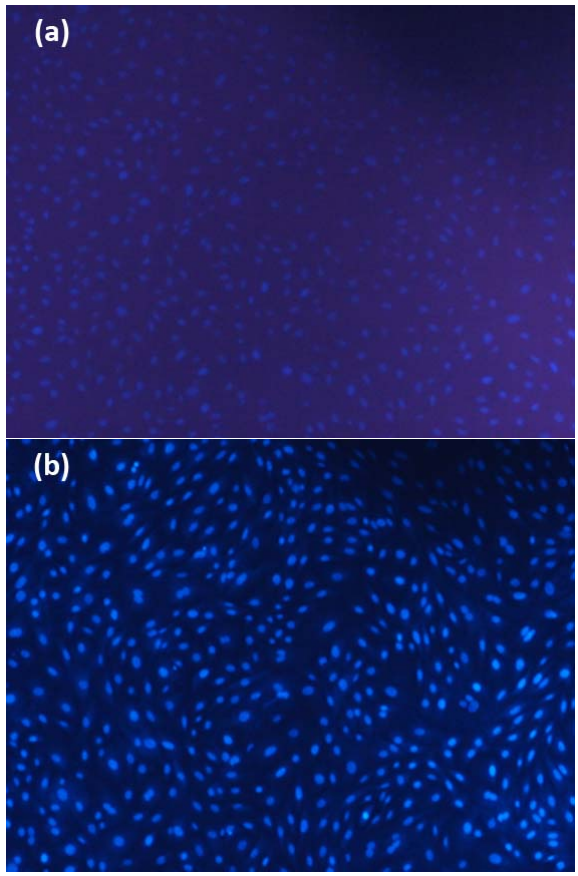

Figure 5.3.2: *Dapi staining for (a) fibroblasts on cartilage scaffolds and (b) on gelatin/collagen coating (control) at third day.*

5.3.2 SEM micrographies

On 22.5% w/v HA scaffolds, cells had a good spreading degree even if it seemed to be not homogeneous (figure. 5.3.3 on the next page). A good proliferation degree and an uniform cell distribution over the entire biomaterial surface were evident on 47.5% HA scaffolds. Furthermore there were a good cell interaction and a good material adhesion (figure 5.3.4 on the facing page). 60% HA scaffolds presented an inhomogeneous surface that led to a reduced interaction with cells

accordingly with a poor cell spreading (figure 5.3.5 on the next page). Increasing HA concentration to 70%, surface showed many hollows. Cells were few and with an elongated form (figure 5.3.6 on the following page). Onto 80% HA scaffolds there was a poor cell-substrate interaction with consequently few cells (figure 5.3.7 on the next page). Cells on 90% HA scaffolds, were not only elongated but they presented some degenerative protrusions (figure 5.3.8 on page 85).

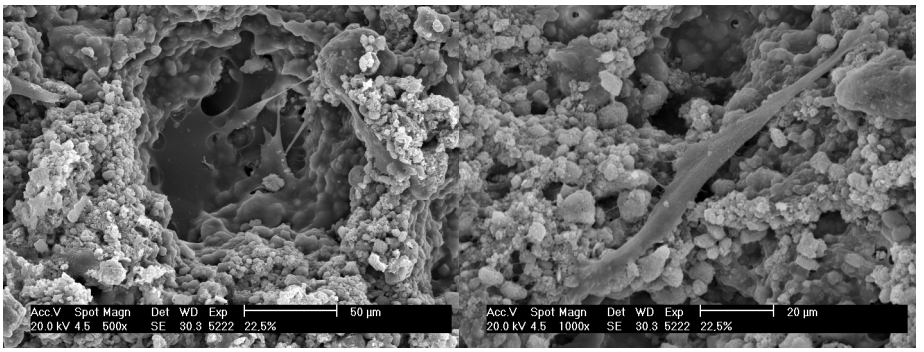

Figure 5.3.3: *SEM of 22.5% HA samples at 500X and 1000X magnification.*

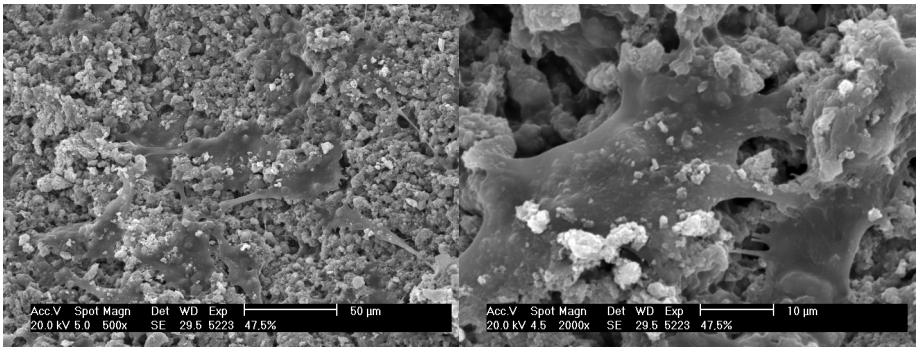

Figure 5.3.4: *SEM of 47.5% HA samples at 500X and 2000X magnification.*

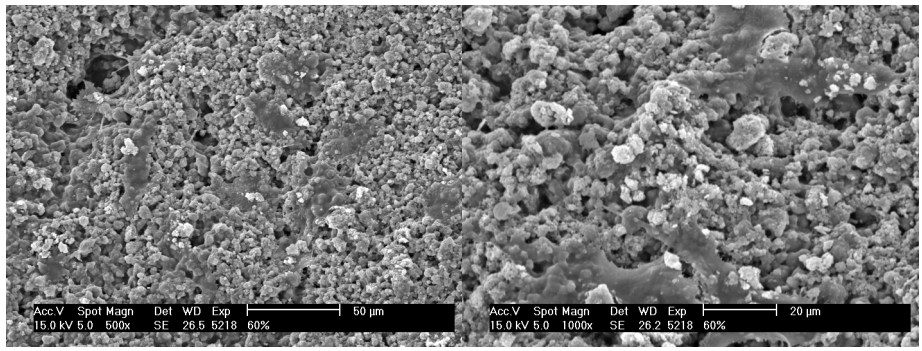

Figure 5.3.5: *SEM of 60% HA samples at 500X and 2000X magnification.*

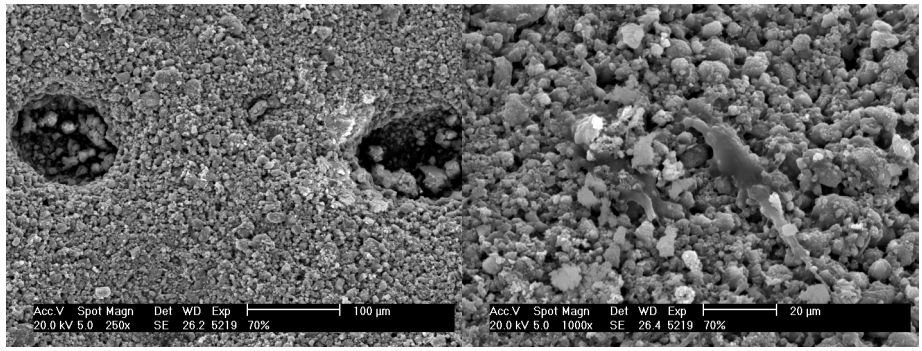

Figure 5.3.6: *SEM of 70% HA samples at 250X and 1000X magnification.*

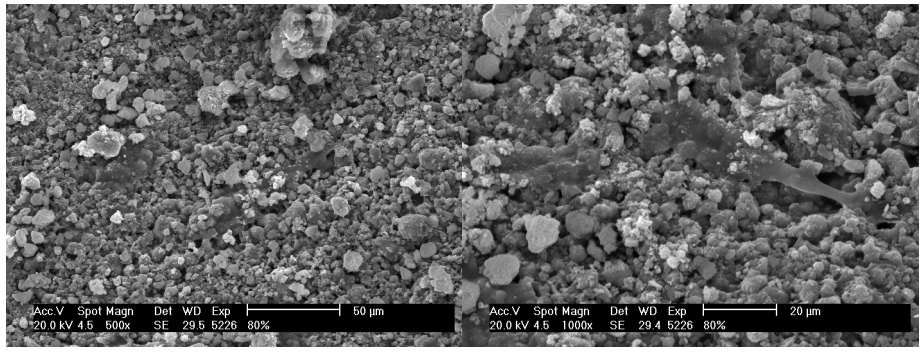

Figure 5.3.7: *SEM of 80% HA samples at 500X and 1000X magnification.*

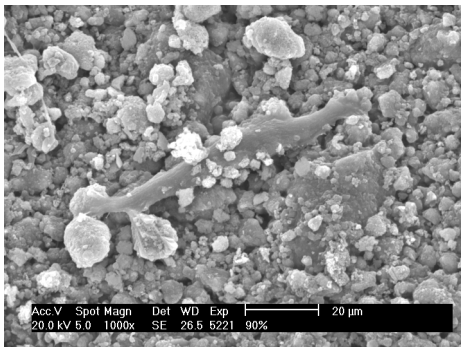

Figure 5.3.8: *SEM of 90% HA samples at 1000X magnification.*

5.3.3 SEM-EDX micrographies

SEM-EDX microanalysis tecnique revealed a different Ca and P distribution in analyzed samples. 60% HA sample had Ca (red in figure) 66% wt, and P (green in figure) 34% wt while 70% HA sample had on surface Ca 71% wt and P 29% wt as showed in figure 5.3.9. Protrusions observed in cells onto 90% HA scaffolds were inclusion of HA confirmed by microanalysis, Ca 69% wt and P 31% wt (figure 5.3.10 on the following page).

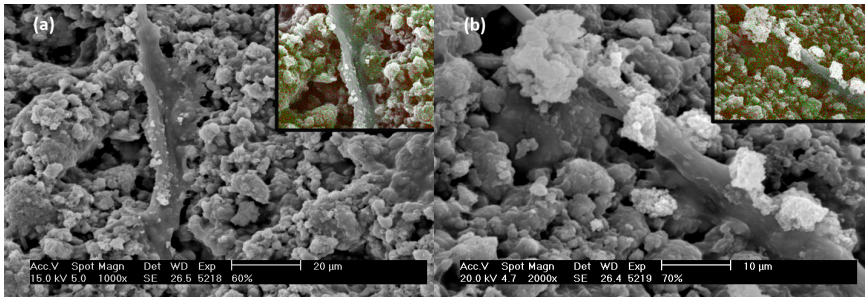

Figure 5.3.9: *SEM-EDX of (a) 60% HA and (b) 70% HA samples showing Ca (red) and P (green) distribution.*

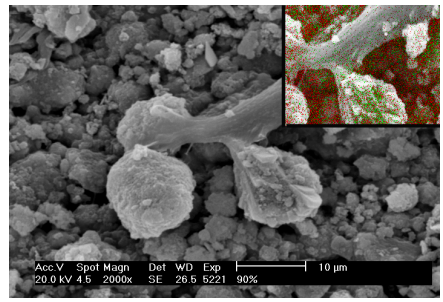

Figure 5.3.10: *SEM-EDX of 90% HA sample showing Ca (red) and P (green) inclusions and distribution.*

5.4 Conclusions

Cartilage biomaterials showed a good biocompatibility, even if cells required a period to adapt to the new substrate. As far as bone subsitute there was a threshold HA concentration, above which the surface roughness becomes unsuited to cells and HA passes from to be bioactive to be toxic. In fact cells had a good spreading and adhesion till 47.5% HA sample, they become suffering from 60% HA samples to degenerate till including HA at 90%. So even if scaffolds containing much than 60% HA, showed a suited Young's modulus to be used as bone substitute, they resulted unfit for cell growth.

6

In vivo tests

Abstract

This chapter will be present in vivo tests of bone and cartilage polymeric systems carried out on Wistar rats. Cartilage damage was performed on cartilage knee while bone defect on femur at diaphysis level. Bone and cartilage regeneration were assessed after 45 days from implantation with in vivo micro-CT and after 3 months with in vivo and ex vivo micro-CT and histology.

6.1 Introduction

In this chapter besides biocompatibility of biomaterials, injectability was tested in animal model. Only some HA concentrations of bone biomaterials were tested *in vivo* and they were chosen on the basis of the most promising Young's modulus. Injectable materials do not require invasive surgery, so they reduce most of the complications normally present in routine surgery. Injectable alginate scaffolds cross-linked with calcium and incorporating chondrocytes, have been studied. These systems induce cartilage repair, but they are unstable and unable to reproduce a functional tissue repair [69]. This response perhaps is due to immunogenic effect of alginate that induces the increase of lymphocytes and anti-alginate antibodies. Synthetic injectable polymers have also been tested as matrixes for chondrocyte grafts, such as polyethylenoxide (PEO) and copoly-

mers with propylene PEO-co-PO (propylene oxide), that have shown a more physiological cartilage regeneration respect to PGA or alginate scaffolds [70]. A novel biocompatible and biodegradable hydrogel comprised of poly(ethylene glycol), gelatin, and genipin, was tested as an injectable biomaterial in combination with a cyanoacrylate-based surgical sealant for cartilage repair[71]. The results demonstrated that the hydrogel is biocompatible and biodegradable, and that the cyanoacrylate-based surgical sealant is a relatively safe option for maintaining the hydrogel in the defect.

6.2 Experimental section

6.2.1 Implantation procedure

Guidelines laid by the "Istituto Superiore di Sanità" for animal testing were followed performed with the approval of the Local Ethical Committee and in accordance with the European Communities Council Directive of 24 November 1986 (86/609/EEC). Surgery was carried out on Wistar rats under deep anesthesia. The patella of left leg was dislocated medially and an osteochondral knee defect was created on femoral ephysis using the tip of tweezers. Cartilage substitute was prepared in sterile condition following the protocol described in chapter 3 and it was injected when the solution became blue (figure 6.2.1). Bone damage of

Figure 6.2.1: *Cartilage biomaterial injenction in rat knee.*

about 5 mm of diameter was produced onto right and left femur (diaphysis) us-

ing a drill, in Wistar anaesthetized rats, involving cortical and spongy bone. The right femur was used as control the other one was treated with bone biomaterial with 70%, 80% and 90% HA (fig. 6.2.2).

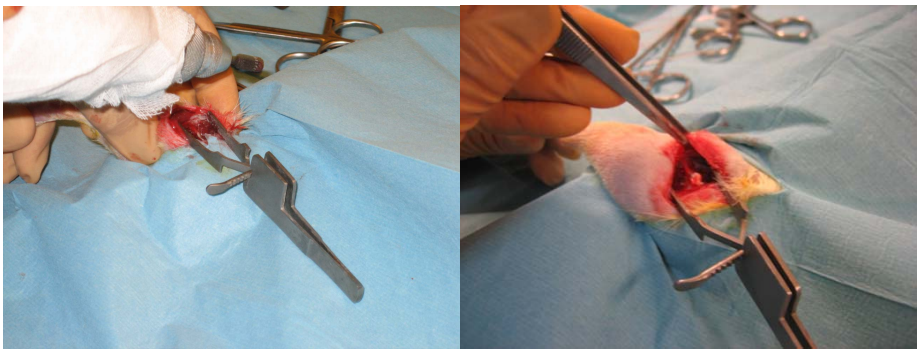

Figure 6.2.2: *Bone biomaterials implantation in left rat femur.*

6.2.2 Micro CT analysis

In vivo micro-CT was performed on anesthetized rats after 45 days and 3 months from implants using The Xalt scanner (X-ray AnimaL Tomograph), a dedicated in vivo cone beam mCT for small animals, designed to provide flexible geometry setup and scanning modality. It was built in the framework of a collaboration between the Institute of Clinical Physiology (IFC-CNR) and the Functional Imaging and Instrumentation Group (FIIG) of the University of Pisa. After *in vivo* µCT at third month, rats were deeply re-anesthetized and euthanized and a high-resolution µCT was performed on explanted femurs.

6.2.3 Histology

Femurs were fixed in phosphate-buffered 4% formaldehyde solution for more than 24h. After fixations, samples were decalcified in 10 ml of electrolytic decalcifying solution (Bio-Optica, Milan, Italy) containing hydrochloric acid and formic acid, for two days. Once that diaphysis lesion was identified it was sampled by performing three cuts perpendicular to the major axis of the bone. Two cuts

were slightly distant from lesion and the other was in the middle of it, in order to obtain two bone cylinders, each containing half lesion. Then cylinders were embedded in paraffin, and a serial of coronal sections thickness of 5 µm were performed. Some sections were stained with eosin and hematoxylin. The same protocol was followed for epiphysis femoral lesion (cartilage damage) with the exception that bone was sectioned orthogonally respect to its major axis and longitudinally through the center of the trochlea to obtain half lesion for each sample.

6.3 Results

6.3.1 *In vivo µCT*

A quantitative analysis was conducted for diaphysis lesions where bone biomaterials were applied. *In vivo* µCT images were elaborated using ImageJ software, and bone volume was considered as bone regeneration parameter at 45 days and 100 days. There was no improvement in bone repair in the left leg (treated) respect to the right leg (control) after 45 days and also after 100 days for all HA concentrations tested as data show in figure 6.3.1. Unfortunaltely there were no data for 90% HA after 45 days, because rats died after first µCT session. While

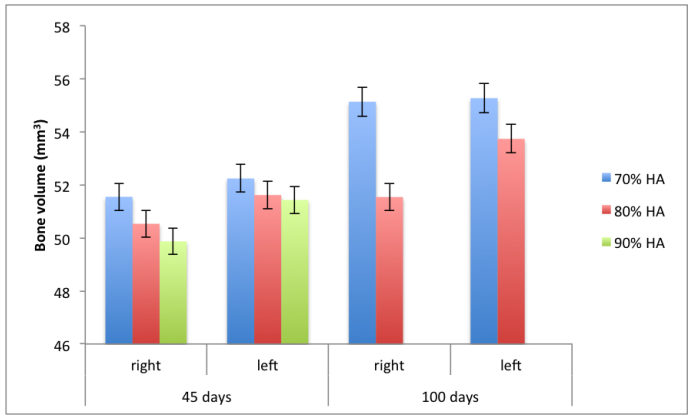

Figure 6.3.1: *Bone volume of left and right legs after 45 days and 100 days.*

physiologic bone regeneration between 45 days and 100 days was evident more in 70% HA rats for both legs than 80% HA. The same analysis was impossible to repeat with cartilage substitutes, because we wanted to see if biomaterial helped cartilage repair (normally cartilage doesn't repair itself) so at the end of experiment we looked at eventually new cartilage in injury site. And even if we wanted to compare cartilage repair between the two temporal spaces, the low resolution of images made the damage difficult to identify. Only after high resolution *ex vivo* µCT was possible to see the damage.

6.3.2 *Ex vivo µCT*

High resolution of images allowed to calculate also bone surface that includes lacunae surface so making the ratio bone volume/bone surface, we had a more reliable data for bone regeneration. In the following table 6.1 we compare this ratio between right leg (control) and left leg (treated).

%HA	Femur	bone volume (BV)/bone surface (BS)
70	Right	0.318
	Left	0.331
80	Right	0.325
	Left	0.317
90*	Right	0.335
	Left	0.326

Table 6.1: *Bone volume, bone surface ratio as parameter for bone regeneration for all HA tested;*reffered to a period inferior to 100 days.*

All values, for both right and left legs were inferior to one and similar among them, which meant that there was no improvement after biomaterial application and that surface of considered bone section was bigger than volume (fig. 6.3.2 on the following page and 6.3.3 on page 93). *Ex vivo* images, showed clearly the epiphysis femoral lesion also after 100 days after cartilage sustitute application (fig. 6.3.4 on the following page).

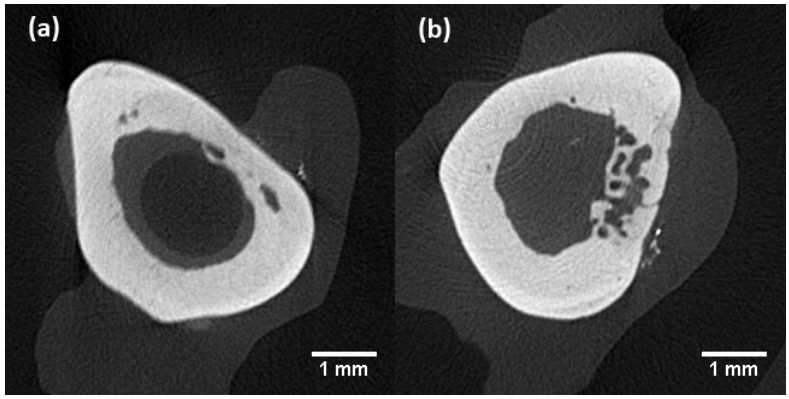

Figure 6.3.2: *Axial plane of (a) right and (b) left femur of rats with 80% HA biomaterial.*

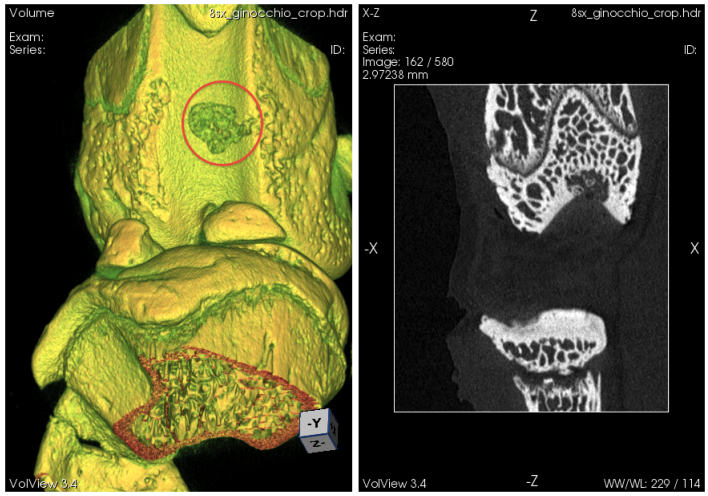

Figure 6.3.4: *Ex vivo high resolution image of cartilage damage after 100 days from biomaterial implant.*

6.3.3 Histology

With regards to macroscopic aspect at diaphysis level it appeared as an area of depression of the bone profile in all femurs (treated and control) figure 6.3.5.

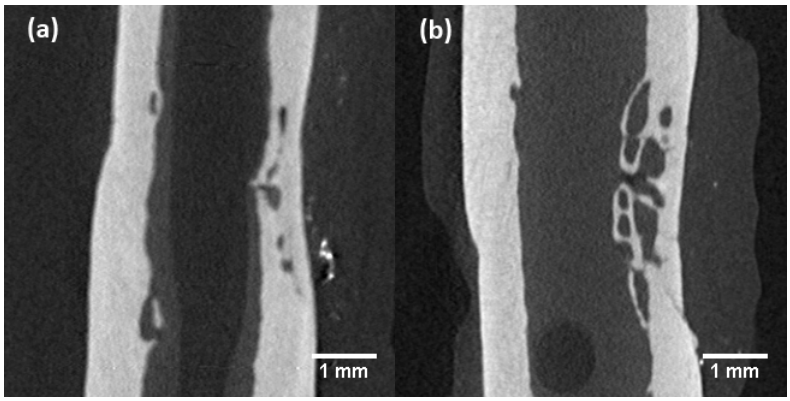

Figure 6.3.3: *Sagittal plane of (a) right and (b) left femur of rats with 80% HA biomaterial.*

Figure 6.3.5: *Macroscopic identification of diaphysis lesion.*

At microscopic level were visible endosteal and periosteal irregularities of reasonable extent. Cortical bone thickness was reduced uniformly (fig. 6.3.8 on the next page) in all samples and were visible medullary spaces, numerous new osteocytes, blood vessels and cement at reversal lines signs of starting bone regeneration (fig. 6.3.6 on the following page). There was no osteoclasts and no inflammation but were visible some Howship lacunae (fig. 6.3.7 on the next page).

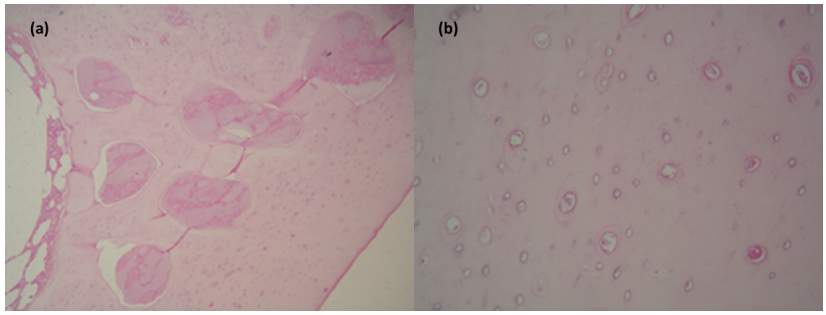

Figure 6.3.6: *Microscopic images: (a) medullary spaces and (b) blood vessels and new osteocytes in cortical bone.*

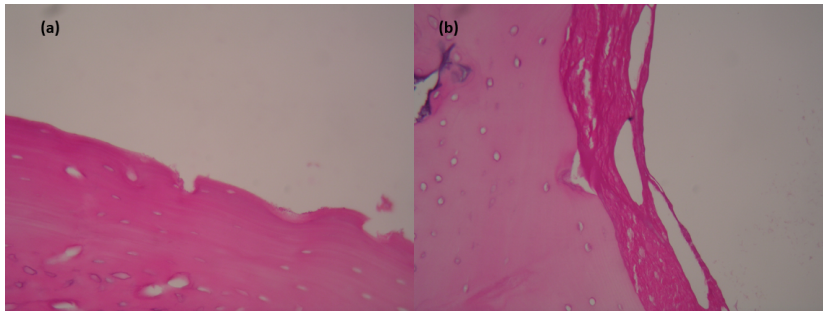

Figure 6.3.7: *(a) Periosteal (left femur) and (b) endosteal (right femur) Howship lacunae.*

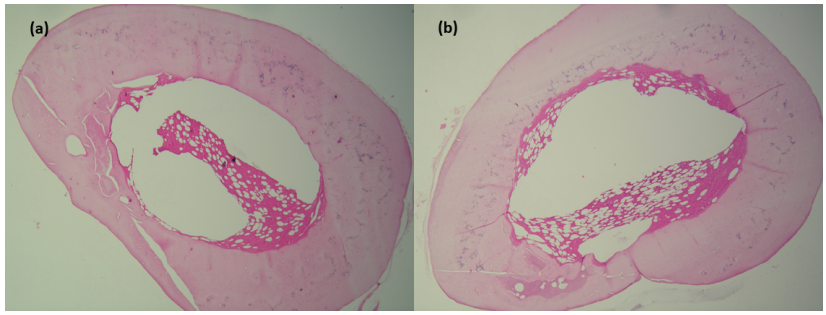

Figure 6.3.8: *(a) Reduced cortical thickness, medullary spaces; (b) irregular endosteal profile.*

Epiphysis femoral lesion at a macroscopic level was evident in the center of the trochlea (fig. 6.3.9). At a microscopic level, cartilage had a damage, with a triangular form involving also cancellous bone. Bone damage was totally filled with fibrous tissue and there were few osteoclasts at this level (fig. 6.3.10). With histology techniques used was impossible to identify remaining biomaterials.

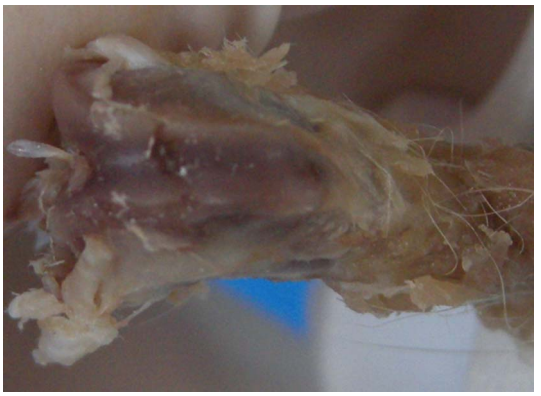

Figure 6.3.9: *Macroscopic identification of epiphysis femoral lesion.*

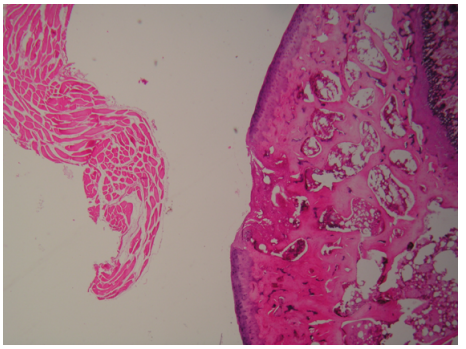

Figure 6.3.10: *Cartilage damage, and cancellous bone replaced with fibrous tissue.*

6.4 Conclusions

Both micro-CT and histology confirmed that bone and cartilage damage after 100 days from implantation of biomaterials were still present. There were no differences between right (control) and left (treated with biomaterial) femurs for all HA concentrations injected. A reason could be that bone biomaterial was ineffective, also considering in vitro data, or simply it didn't remain in contact with lesion enought time to be colonized by cells. Important was the absence of imflammation state. The same consideration can be applied to cartilage. Further, because of the non invasive surgery technique to create a cartilage lesion used in these experiments, was impossible to assess the inital damage and to follow the progress of regeneration. From histology performed at 100 days, we knew that the damage involved also bone and that the physiologic cartilage repair started, that is replacement of tissue with fibrous one, and so that there was no new cartilage tissue.

Conclusions

The aim of this research was to test some biomaterials as bone and cartilage sustitutes. Biomaterials studied were a polymeric mixture of hydrogel, gelatin and collagen type I, that as natural substances are biocompatible, biodegradable and chemo-attractor. The main problem with the use of hydrogel is their rapid dissolution in an aqueous environment, so a crosslinking agent was necessary. Genipin was chosen, because it is natural, it ensures an efficient reaction and it is much less toxic than the other crosslinkers commonly used. In literature, there were many mechanical and chemical data, about gelatin and genipin scaffolds, but nothing with the inclusion of collagen. So fundamental was the characterization of reaction (rate constant, diffusion coefficient and crosslinking degree). From data collected, with particular attention to GP toxicity, its best concentration was decided for cartilage and bone scaffolds. Equally important were mechanical tests performed on cartilage scaffolds at different GP concentrations, and on bone scaffolds at different HA concentrations. Elastic modulus of cartilage scaffolds calculated did not mimic that of native tissue but the presence of chemo-attractors (collagen) within them should help to produce fast cell colonization. Mechanical test results helped the choice of the best preparation protocol for bone scaffolds. Their Young's modulus could be adjust changing HA concentration till reaching the cancellous bone modulus after scaffolds dehydration.

The same scaffolds were used to realise discrete gradient samples, simply stacking two or more homogeneous HA scaffolds, to reflect more accurately phisilogycal bone structure. Anisotropy, one mechanical bone feature, was verified particular for multilayered scaffolds. Considering that those biomaterials should be used after a trauma, and that it involves a pH variation, possible elastic modulus changes at pH 5, 6, 7, 8 were investigated only for homogeneous scaffolds. In fact modulus respect to physiologic pH, decreased in acid condition (pH 5), while it increase at slightly basic pH. After mechanical studies, preliminary in vitro tests were performed to assess biocompatibility of polymeric systems. Primary fibroblasts seeded onto cartilage scaffolds showed an increasing viability across 3 days, till reaching control value at the end of experiment. Bone scaffolds were seeded with MG-63 human osteoblast-like cells, and they were analysed with SEM and SEM-EDX. A good cells spreading and adhesion was verified only for low HA concentration, starting from 60% HA cells became suffering to degenerate till including HA at 90%. In spite of these results, high concentration HA biomaterials, togheter with cartilage one, were tested *in vivo* as injectable. Lesions were made on femur rats, where biomaterials were applied. Bone and cartilage regeneration was verified after 45 days and after 100 days with *in vivo* micro CT analysis. Animals were sacrified at the end of experiment (100 days) and *ex vivo* micro CT (high resolution micro CT) and histology were performed. Both analyses confirmed that there was no improvement in bone regenaration in the treated femur respect to the physiologic bone repair. The osteochondral lesion was partially repaired with fibrous tissue and not with new cartilage. Biomaterials can't be label as ineffective with absolute certainty, because it was impossible to detect them at 45 days with μCT and also at 100 days with histology. Since HA usually needs many years to be degradeted, probably biomaterial didn't remain onto lesion enough time to be colonized by cells so it should be injected when it will assume a higher viscosity, typical of an advanced stage of crosslinking reaction. Biomaterials formulated and tested in this research, show promising mechanical properties but they need more *in vivo* investigations, particular for bone scaffolds at low HA concentrations.

Author Publications

International Journals

G. Mattei, F. Montemurro, M. Mattioli-Belmonte, G. Vozzi. Novel injectable hydrogel scaffold for cartilage repair based on natural polymers. *Journal of Osteology and Biomaterials vol I,* number 3-2010, 153-161. G. Vozzi, T. Lenzi,

F. Montemurro, C. Pardini, F. Vaglini, A. Ahluwalia. A Novel Method to Produce Immobilised Biomolecular Concentration Gradients to Study Cell Activities: Design and Modelling; *Molecular biotechnology* (2011)

C. Jelen, G. Mattei, F. Montemurro, C. De Maria, M. Mattioli Belmonte, G. Vozzi. Bone Scaffolds with homogeneous and discrete gradient mechanical properties. *Material Science and Engineering part C* submitted

A. Urciuolo, M. Quarta, V. Morbidoni, F. Gattazzo, P. Grumati, S. Molon, F. Montemurro, F.S. Tedesco, G. Cossu, G. Vozzi, T.A. Rando, P. Bonaldo. Collagen VI is a key component of satellite cell niche required for muscle regeneration, *Nature Medicine* submitted.

M. Pifferi, A. Bush, F. Montemurro, G. Pioggia, M. Piras, G. Tartarisco, M. Di Cicco, I. Chinellato, A.M. Cangiotti, and A.L. Boner; Rapid diagnosis of

Primary Ciliary Dyskinesia: cell culture and soft computing analysis. *European Respiratory Journal* submitted.

Proceedings and Abstracts

Pifferi M, Ragazzo V, Vozzi G, Cangiotti A, Mantovani G, Montemurro F, Di Cicco M, Goldsztajn W, Barrani M, Ahluwalia A, Macchia P. Le colture dell'epitelio ciliato prelevato mediante brushing nasale nella diagnosi della discinesia ciliare primaria, *Discinesie ciliarie e malattie respiratorie croniche del bambino: dalla diagnosi differenziale alla qualità della vita*, 14-15 Marzo 2008.

F. Montemurro, T. Lenzi, C. Pardini, G. Vozzi, F. Vaglini, A. Ahluwalia, Generation of immobilised gradients without microfluidics for adhesion of neural cells, *TERMIS 2008 Porto*, Portugal

F. Montemurro, T. Lenzi, C. Pardini, G. Vozzi, F. Vaglini, A. Ahluwalia, "An immobilizer gradient generator for spatially differentiated adhesion of neurons", *Congresso Nazionale di Bioingegneria 2008* Atti, pp.387-388

G. Mattei, F. Montemurro, A. Ahluwalia, G. Vozzi, "Sviluppo e caratterizzazione meccanica di scaffold a base di collagene per la rigenerazione della cartilagine", *Congresso Nazionale Biomateriali 2008*, Follonica (Italy), 17-19 September 2008. Abstract p. 75

A. Moschetti; F. Montemurro; C. De Maria; F. Vozzi; A. Ahluwalia; G. Vozzi, "In silico" model of hepatic metabolism of Diclofenac, *Congresso Nazionale di Bioingegneria 2010* Atti

A.Morachioli; G. Vozzi; F. Montemurro, Soft-MI scaffold for tissue engineering applications, *Congresso Nazionale di Bioingegneria 2010* Atti

S. Romiti; G. Vozzi; C. De Maria; F. Montemurro, Mechanical characterization of polymer cartilage scaffold at different pH, *Congresso Nazionale di Bioingegneria 2010* Atti

A. Tirella, F. Montemurro, B. Vinci, F. Vozzi, G. Vozzi, D. Sassano, T. Sandri, L. Cognolato, and A. Ahluwalia, Site Specific Nano-Tuning of Scaffolds Using Inkjet Printing, *NIP Conference*, Austin, Texas / September 19–23, 2010

F. Vozzi, F. Montemurro, M.A. Guzzardi, C. Domenici, A. Ahluwalia, Predicting cytotoxic response to drugs: The multi-compartmental bioreactor system, *IUTOX 2010 XII International Congress of Toxicolog*, Barcelona-Spain 19–23 July 2010 Toxicology Letters p. 196

Bibliography

[1] Hunter, W, "Of the structure and disease of articulating cartilages. 1743," *Clin Orthop Relat Res*, , no. 317, pp. 3–6, Aug 1995

[2] Kalson, N S, Gikas, P D, and Briggs, T W R, "Current strategies for knee cartilage repair," *Int J Clin Pract*, volume 64, no. 10, pp. 1444–52, Sep 2010

[3] Cheung, H S, Lynch, K L, Johnson, R P, and Brewer, B J, "In vitro synthesis of tissue-specific type II collagen by healing cartilage. I. Short-term repair of cartilage by mature rabbits," *Arthritis Rheum*, volume 23, no. 2, pp. 211–219, Feb 1980

[4] Redman, SN, Oldfield, SF, Archer, CW, *et al.*, "Current strategies for articular cartilage repair," *Eur Cell Mater*, volume 9, pp. 23–32, 2005

[5] Shapiro, F., Koide, S., Glimcher, MJ, *et al.*, "Cell origin and differentiation in the repair of full-thickness defects of articular cartilage." *The Journal of bone and joint surgery American volume*, volume 75, no. 4, p. 532, 1993

[6] Buckwalter, JA *et al.*, "Articular cartilage: injuries and potential for healing." *The Journal of orthopaedic and sports physical therapy*, volume 28, no. 4, p. 192, 1998

[7] Knutsen, G, Drogset, J O, Engebretsen, L, Grontvedt, T, Isaksen, V, Ludvigsen, T C, Roberts, S, Solheim, E, Strand, T, and Johansen, O, "A randomized trial comparing autologous chondrocyte implantation with microfracture. Findings at five years," *J Bone Joint Surg Am*, volume 89, no. 10, pp. 2105–2112, Oct 2007

[8] Langer, R and Vacanti, J P, "Tissue engineering," *Science*, volume 260, no. 5110, pp. 920–926, May 1993

[9] Mano, J F and Reis, R L, "Osteochondral defects: present situation and tissue engineering approaches," *J Tissue Eng Regen Med*, volume 1, no. 4, pp. 261–273, Jul-Aug 2007

[10] Thomson, R., Wake, M., Yaszemski, M., and Mikos, A., "Biodegradable polymer scaffolds to regenerate organs," *Biopolymers Ii*, pp. 245–274, 1995

[11] Einhorn, T.A., "The cell and molecular biology of fracture healing," *Clinical orthopaedics and related research*, volume 355, p. S7, 1998

[12] Ferguson, C., Alpern, E., Miclau, T., and Helms, J.A., "Does adult fracture repair recapitulate embryonic skeletal formation?" *Mechanisms of development*, volume 87, no. 1-2, pp. 57–66, 1999

[13] Bauer, T.W. and Muschler, G.F., "Bone graft materials: an overview of the basic science," *Clinical orthopaedics and related research*, volume 371, p. 10, 2000

[14] Ahlmann, E., Patzakis, M., Roidis, N., Shepherd, L., and Holtom, P., "Comparison of anterior and posterior iliac crest bone grafts in terms of harvest-site morbidity and functional outcomes," *The Journal of Bone and Joint Surgery American*, volume 84, no. 5, pp. 716–720, 2002

[15] ST John, T.A., Vaccaro, A.R., Sah, A.P., Schaefer, M., Berta, S.C., Albert, T., and Hilibrand, A., "Physical and monetary costs associated with autogenous bone graft harvesting," *The American journal of orthopedics*, volume 32, no. 1, pp. 18–23, 2003

[16] Giannoudis, P.V., Dinopoulos, H., and Tsiridis, E., "Bone substitutes: an update," *Injury*, volume 36, no. 3, pp. S20–S27, 2005

[17] Ripamonti, U., "Osteoinduction in porous hydroxyapatite implanted in heterotopic sites of different animal models," *Biomaterials*, volume 17, no. 1, pp. 31–35, 1996

[18] Ducheyne, P. and Qiu, Q., "Bioactive ceramics: the effect of surface reactivity on bone formation and bone cell function," *Biomaterials*, volume 20, no. 23-24, pp. 2287–2303, 1999

[19] Michael W, C. and Robert, B., "Treatment of Acute Fractures with a Collagen-Calcium Phosphate Graft Material. A Randomized Clinical Trial," *The Journal of Bone and Joint Surgery American*, volume 79, no. 4, pp. 495–502, 1997

[20] Holmes, R.E., "Bone regeneration within a coralline hydroxyapatite implant," *Plastic and Reconstructive Surgery*, volume 63, no. 5, p. 626, 1979

[21] Oh, S.H., Park, I.K., Kim, J.M., and Lee, J.H., "In vitro and in vivo characteristics of PCL scaffolds with pore size gradient fabricated by a centrifugation method," *Biomaterials*, volume 28, no. 9, pp. 1664–1671, 2007

[22] Huang, J., Silvio, L.D.I., Wang, M., Tanner, KE, and Bonfield, W., "In vitro mechanical and biological assessment of hydroxyapatite-reinforced polyethylene composite," *Journal of Materials Science Materials in Medicine*, volume 8, no. 12, pp. 775–779, 1997

[23] Oonishi, H., "Orthopaedic applications of hydroxyapatite," *Biomaterials*, volume 12, no. 2, pp. 171–178, 1991

[24] Li, P., Yang, Q., Zhang, F., and Kokubo, T., "The effect of residual glassy phase in a bioactive glass-ceramic on the formation of its surface apatite layer in vitro," *Journal of Materials Science Materials in Medicine*, volume 3, no. 6, pp. 452–456, 1992

[25] Mano, J.F., Sousa, R.A., Boesel, L.F., Neves, N.M., and Reis, R.L., "Bioinert, biodegradable and injectable polymeric matrix composites for hard tissue replacement: state of the art and recent developments," *Composites Science and Technology*, volume 64, no. 6, pp. 789–817, 2004

[26] Logeart-Avramoglou, D., Anagnostou, F., Bizios, R., and Petite, H., "Engineering bone: challenges and obstacles," *Journal of cellular and molecular medicine*, volume 9, no. 1, pp. 72–84, 2005

[27] Rose PJ, Mark HF, Bikales NM Overberger CG Menges G Kroschwitz JI, *Encyclopedia of polymer science and engineering*, volume 7, 2nd edition, 1987

[28] Pezron I, Djabourov M, Leblond J, *Polymer*, chapter 32, pp. 3201–10, 1991

[29] Fakirov, S., Sarac, Z., Anbar, T., Boz, B., Bahar, I., Evstatiev, M., Apostolov, AA, Mark, JE, and Kloczkowski, A., "Mechanical properties and transition temperatures of cross-linked oriented gelatin," *Colloid amp Polymer Science*, volume 274, no. 4, pp. 334–341, 1996

[30] Yao, C.H., Sun, J.S., Lin, F.H., Liao, C.J., and Huang, C.W., "Biological effects and cytotoxicity of tricalcium phosphate and formaldehyde crosslinked gelatin composite," *Materials chemistry and physics*, volume 45, no. 1, pp. 6–14, 1996

[31] Lodish, H. and Darnell, J.E., *Molecular cell biology*, volume 5, Wiley Online Library, 2000

[32] Elsdale, T. and Bard, J., "Collagen substrata for studies on cell behavior," *The Journal of cell biology*, volume 54, no. 3, pp. 626–637, 1972

[33] Nishi, C., Nakajima, N., and Ikada, Y., "In vitro evaluation of cytotoxicity of diepoxy compounds used for biomaterial modification," *Journal of biomedical materials research*, volume 29, no. 7, pp. 829–834, 1995

[34] Lohre, J.M., Baclig, L., Wickham, E., Guida, S., Farley, J., Thyagarajan, K., Tu, R., and Quijano, RC, "Evaluation of epoxy ether fixed bovine arterial

grafts for mutagenic potential," *ASAIO journal*, volume 39, no. 2, p. 106, 1993

[35] Sung, H.W., Huang, R.N., Huang, L.L.H., and Tsai, C.C., "In vitro evaluation of cytotoxicity of a naturally occurring cross-linking reagent for biological tissue fixation," *Journal of Biomaterials Science Polymer Edition*, volume 10, no. 1, pp. 63–78, 1999

[36] Sung, H.W., Chang, Y., Chiu, C.T., Chen, C.N., and Liang, H.C., "Mechanical properties of a porcine aortic valve fixed with a naturally occurring crosslinking agent," *Biomaterials*, volume 20, no. 19, pp. 1759–1772, 1999

[37] Sung, H.W., Chen, C.N., Huang, R.N., Hsu, J.C., and Chang, W.H., "In vitro surface characterization of a biological patch fixed with a naturally occurring crosslinking agent," *Biomaterials*, volume 21, no. 13, pp. 1353–1362, 2000

[38] Sung, H.W, Huang, R.N, Huang, L.L.H, Tsai, C.C, and Chiu, C.T, "Feasibility study of a natural crosslinking reagent for biological tissue fixation," *Journal of biomedical materials research Part A*, volume 42, no. 4, pp. 560–567, 1998

[39] Tseng, T.H., Chu, C.Y., Huang, J.M., Shiow, S.J., and Wang, C.J., "Crocetin protects against oxidative damage in rat primary hepatocytes," *Cancer letters*, volume 97, no. 1, pp. 61–67, 1995

[40] Yamamoto, M., Miura, N., Ohtake, N., Amagaya, S., Ishige, A., Sasaki, H., Komatsu, Y., Fukuda, K., Ito, T., and Terasawa, K., "Genipin, a metabolite derived from the herbal medicine Inchin-ko-to, and suppression of Fas-induced lethal liver apoptosis in mice," *Gastroenterology*, volume 118, no. 2, pp. 380–389, 2000

[41] Yamazaki, M., Sakura, N., Chiba, K., and Mohri, T., "Prevention of the neurotoxicity of the amyloid beta protein by genipin," *Biological amp pharmaceutical bulletin*, volume 24, no. 12, pp. 1454–1455, 2001

[42] Koo, Hye-Jin, Song, Yun Seon, Kim, Hee-Jeong, Lee, Yong-Ha, Hong, Sung-Min, Kim, Su-Jung, Kim, Byung-Chul, Jin, Changbae, Lim, Chang-Jin, and

Park, Eun-Hee, "Antiinflammatory effects of genipin, an active principle of gardenia," *Eur J Pharmacol*, volume 495, no. 2-3, pp. 201–8, Jul 2004

[43] Lima, E G, Tan, A R, Tai, T, Marra, K G, DeFail, A, Ateshian, G A, and Hung, C T, "Genipin enhances the mechanical properties of tissue-engineered cartilage and protects against inflammatory degradation when used as a medium supplement," *J Biomed Mater Res A*, volume 91, no. 3, pp. 692–700, Dec 2009

[44] Yuan, H., Kurashina, K., de Bruijn, J.D., Li, Y., De Groot, K., and Zhang, X., "A preliminary study on osteoinduction of two kinds of calcium phosphate ceramics," *Biomaterials*, volume 20, no. 19, pp. 1799–1806, 1999

[45] Du, C., Cui, FZ, Zhu, XD, and De Groot, K., "Three-dimensional nano-HAp/collagen matrix loading with osteogenic cells in organ culture," *Journal of biomedical materials research*, volume 44, no. 4, pp. 407–415, 1999

[46] Rezwan, K., Chen, QZ, Blaker, JJ, and Boccaccini, A.R., "Biodegradable and bioactive porous polymer/inorganic composite scaffolds for bone tissue engineering," *Biomaterials*, volume 27, no. 18, pp. 3413–3431, 2006

[47] Kikawa, T., Kashimoto, O., Imaizumi, H., Kokubun, S., and Suzuki, O., "Intramembranous bone tissue response to biodegradable octacalcium phosphate implant," *Acta biomaterialia*, volume 5, no. 5, pp. 1756–1766, 2009

[48] Dong, Guo-Chung, Chen, Hueih Min, and Yao, Chun-Hsu, "A novel bone substitute composite composed of tricalcium phosphate, gelatin and drynaria fortunei herbal extract," *Journal of biomedical materials research Part A*, volume 84, no. 1, pp. 167–77, Jan 2008

[49] Mi, F.L., Sung, H.W., and Shyu, S.S., "Synthesis and characterization of a novel chitosan-based network prepared using naturally occurring crosslinker," *Journal of Polymer Science Part A Polymer Chemistry*, volume 38, no. 15, pp. 2804–2814, 2000

[50] Liang, H.C., Chang, W.H., Liang, H.F., Lee, M.H., and Sung, H.W., "Crosslinking structures of gelatin hydrogels crosslinked with genipin or a

water-soluble carbodiimide," *Journal of applied polymer science*, volume 91, no. 6, pp. 4017–4026, 2004

[51] Touyama, R, Takeda, Y, Inoue, K, Kawamura, I, Yatsuzuka, M, Ikumoto, T, Shingu, T, Yokoi, T, and Inouye, H, "Studies on the blue pigments produced from genipin and methylamine. I: Structures of the brownish-red pigments, intermediates leading to the blue pigments," *Chemical and pharmaceutical bulletin*, volume 42, no. 3, pp. 668–673, 1994

[52] Butler, M.F., Ng, Y.F., and Pudney, P.D.A., "Mechanism and kinetics of the crosslinking reaction between biopolymers containing primary amine groups and genipin," *Journal of Polymer Science Part A Polymer Chemistry*, volume 41, no. 24, pp. 3941–3953, 2003

[53] Mi, FL, Shyu, SS, and Peng, CK, "Characterization of ring-opening polymerization of genipin and pH-dependent cross-linking reactions between chitosan and genipin," *Journal of Polymer Science A Polymer Chemistry Edition*, volume 43, no. 10, pp. 1985–2000, 2005

[54] Udenfriend, S, Stein, S, Böhlen, P, Dairman, W, Leimgruber, W, and Weigele, M, "Fluorescamine: a reagent for assay of amino acids, peptides, proteins, and primary amines in the picomole range," *Science*, volume 178, no. 63, pp. 871–2, Nov 1972

[55] Hoffman, A.S., "Hydrogels for biomedical applications," *Advanced drug delivery reviews*, volume 54, no. 1, pp. 3–12, 2002

[56] Elisseeff, J., McIntosh, W., Anseth, K., Riley, S., Ragan, P., and Langer, R., "Photoencapsulation of chondrocytes in poly (ethylene oxide)-based semi-interpenetrating networks," *Journal of Biomedical Materials Research*, volume 51, no. 2, pp. 164–171, 2000

[57] Sharma, B., Williams, C.G., Khan, M., Manson, P., and Elisseeff, J.H., "In vivo chondrogenesis of mesenchymal stem cells in a photopolymerized hydrogel," *Plastic and reconstructive surgery*, volume 119, no. 1, p. 112, 2007

[58] Leong, KF, Cheah, CM, and Chua, CK, "Solid freeform fabrication of three-dimensional scaffolds for engineering replacement tissues and organs," *Biomaterials*, volume 24, no. 13, pp. 2363–2378, 2003

[59] Marzec, E. and Pietrucha, K., "The effect of different methods of cross-linking of collagen on its dielectric properties," *Biophysical chemistry*, volume 132, no. 2-3, pp. 89–96, 2008

[60] Liu, BS, Yao, CH, Chen, YS, and Hsu, SH, "In vitro evaluation of degradation and cytotoxicity of a novel composite as a bone substitute," *J Biomed Mater Res*, volume 67, no. 4, pp. 1163–1169, 2003

[61] Schwartz, MH, Leo, PH, and Lewis, JL, "A microstructural model for the elastic response of articular cartilage," *Journal of biomechanics*, volume 27, no. 7, pp. 865–873, 1994

[62] Miyamoto, Y., *Functionally graded materials: design, processing, and applications*, number 5, Chapman & Hall, 1999

[63] Dillow, A.K., Lowman, A.M., *et al.*, *Biomimetic materials and design: biointerfacial strategies, tissue engineering, and targeted drug delivery*, CRC Press, 2002

[64] Prendergast, PJ, "Bone prostheses and implants," *Bone mechanics handbook*, pp. 35–1, 2001

[65] Väänänen, H K and Horton, M, "The osteoclast clear zone is a specialized cell-extracellular matrix adhesion structure," *J Cell Sci*, volume 108 (Pt 8), pp. 2729–2732, Aug 1995

[66] Vaananen, HK, Zhao, H., Mulari, M., and Halleen, J.M., "The cell biology of osteoclast function," *Journal of cell science*, volume 113, no. 3, p. 377, 2000

[67] Sung, HW, Huang, RN, Huang, LLH, Tsai, CC, and Chiu, CT, "Feasibility study of a natural crosslinking reagent for biological tissue fixation," *J Biomed Mater Res*, volume 42, no. 4, 1998

[68] Huang, L.L.H., Sung, H.W., Tsai, C.C., and Huang, D.M., "Biocompatibility study of a biological tissue fixed with a naturally occurring crosslinking reagent," *Journal of biomedical materials research*, volume 42, no. 4, pp. 568–576, 1998

[69] Paige, K.T., Cima, L.G., Yaremchuk, M.J., Schloo, B.L., Vacanti, J.P., and Vacanti, C.A., "De novo cartilage generation using calcium alginate-chondrocyte constructs," *Plastic and reconstructive surgery*, volume 97, no. 1, p. 168, 1996

[70] Sims, C.D., Butler, P.E.M., Casanova, R., Lee, B.T., Randolph, M.A., Lee, WP, Vacanti, C.A., and Yaremchuk, M.J., "Injectable cartilage using polyethylene oxide polymer substrates," *Plastic and reconstructive surgery*, volume 98, no. 5, p. 843, 1996

[71] Miljkovic, Natasa D, Lin, Yen-Chih, Cherubino, Mario, Minteer, Danielle, and Marra, Kacey G, "A novel injectable hydrogel in combination with a surgical sealant in a rat knee osteochondral defect model," *Knee Surg Sports Traumatol Arthrosc*, volume 17, no. 11, pp. 1326–31, Nov 2009